

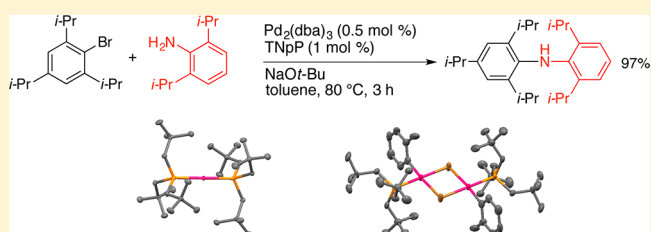
Trineopentylphosphine: A Conformationally Flexible Ligand for the Coupling of Sterically Demanding Substrates in the Buchwald–Hartwig Amination and Suzuki–Miyaura Reaction

Steven M. Raders, Jane N. Moore, Jacquelynn K. Parks, Ashley D. Miller, Thomas M. Leißing, Steven P. Kelley, Robin D. Rogers, and Kevin H. Shaughnessy*

Department of Chemistry, The University of Alabama, Box 870336, Tuscaloosa, Alabama 35487-0336, United States

S Supporting Information

ABSTRACT: Trineopentylphosphine (TNpP) in combination with palladium provides a highly effective catalyst for the Buchwald–Hartwig coupling of sterically demanding aryl bromides and chlorides with sterically hindered aniline derivatives. Excellent yields are obtained even when both substrates include 2,6-diisopropyl substituents. Notably, the reaction rate is inversely related to the steric demand of the substrates. X-ray crystallographic structures of Pd(TNpP)₂, [Pd(4-*t*-Bu-C₆H₄)(TNpP)(μ-Br)]₂, and [Pd(2-Me-C₆H₄)(TNpP)(μ-Br)]₂ are reported. These structures suggest that the conformational flexibility of the TNpP ligand plays a key role in allowing the catalyst to couple hindered substrates. The Pd/TNpP system also shows good activity for the Suzuki coupling of hindered aryl bromides.



INTRODUCTION

Palladium-catalyzed carbon–carbon and carbon–heteroatom bond-forming reactions are one of the most powerful methodologies for the synthesis of natural products, pharmaceuticals, and fine chemicals.¹ Of the family of Pd-catalyzed cross-coupling reactions, the Buchwald–Hartwig amination and Suzuki–Miyaura cross-coupling reactions have been shown to be particularly useful for the synthesis of C–N and C–C bonds, respectively. These reactions are favored because of their ease of operation and high degree of generality.

The Buchwald–Hartwig coupling of aryl halides or pseudohalides with nitrogen nucleophiles is a powerful tool for the synthesis of pharmaceuticals and agricultural materials.² Typically, the Buchwald–Hartwig amination is preferred to classical C–N bond-forming methodologies, such as nucleophilic aromatic substitution, reductive amination, and nitration followed by reduction,³ and Cu-catalyzed amination reactions⁴ because of its high functional group tolerance, single-step procedure, commercially available starting materials, and mild reaction conditions. Sterically demanding, electron-rich ligands, such as trialkylphosphines,⁵ dialkylarylyphosphines (Buchwald ligands),^{2c} bicyclic triaminophosphines (Verkade’s superbases),⁶ *N*-heterocyclic carbenes,⁷ oxaphosphole ligands,⁸ and chelating phosphines,⁹ have been shown to provide highly efficient catalysts in the C–N bond formation.

The Suzuki–Miyaura cross-coupling is an extensively studied synthetic methodology for C–C bond formation owing to the advantages of this reaction over other C–C bond-forming reactions, such as the Negishi (organozinc), Kumada (organomagnesium), Hiyama (organosiloxane), and Stille (organotin)

couplings.^{1a,b,7e,10} The commonly used organoboron reagents are typically insensitive to air and moisture, thermally stable, and tolerate a wide variety of functional groups.¹¹ Although efficient ligand-free catalyst systems have been reported,¹² an ancillary ligand greatly enhances the efficiency of the catalyst. Again, sterically demanding, electron-rich ligands, such as dialkylarylyphosphines,¹³ trialkylphosphines,^{5,14} and *N*-heterocyclic carbenes,^{7c,e} have proven to be particularly useful.

Despite significant study, there remains much to be learned about the interplay of steric and electronic properties of the ligands in these reactions.¹⁵ Recently, our group reported that neopentylphosphines are effective ligands in a variety of palladium-catalyzed cross-coupling reactions.¹⁶ Di(*tert*-butyl)neopentylphosphine (DTBNpP, Figure 1) provides catalysts with comparable or improved activity for C–N and C–C bond-forming reactions of aryl bromides to tri(*tert*-butyl)phosphine (TTBP), while *tert*-butyldineopentylphosphine (TBDNpP) and trineopentylphosphine (TNpP) give less active catalysts at ambient temperature. The DTBNpP-based system gives a

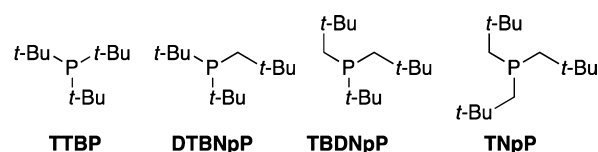


Figure 1. Neopentylphosphine ligands.

Received: February 28, 2013

Published: May 2, 2013

somewhat less active catalyst than TTBP for the coupling of aryl chlorides, however.

The neopentyl group provides a different set of electronic and steric effects than that of a *tert*-butyl group. The *tert*-butyl substituent provides a fairly constant steric influence as it rotates about the P–C bond. In contrast, the steric impact of the neopentyl substituent varies significantly as the M–P–C–C dihedral angle ranges from 0° (maximum steric effect) to 180° (minimal steric influence). Tolman estimated that TNpP and TTBP had similar cone angles (180° and 182°, respectively).¹⁷ These values were measured from the least sterically demanding conformation for each ligand. Solid cone-angles obtained from DFT-optimized, gas-phase Pd(PR₃) structures predicted that ligand cone angles increased with the addition of neopentyl groups (TTBP (194°) < DTBNpP (198°) < TBDNpP (210°) < TNpP (227°)).^{16a} In these calculated structures, the Pd–P–C–C dihedral angle of the neopentyl substituents was small, resulting in the neopentyl group exerting maximal steric influence. The solid-state structure of Pd(DTBNpP)₂ adopts a similar conformation in which the Pd–P–C–C angle is 0.3(1)°.^{16c}

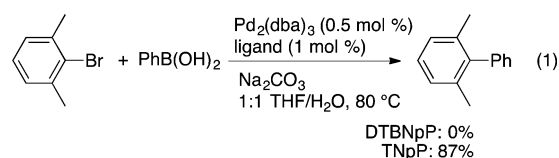
Electronically, the neopentyl substituent would be expected to have a smaller inductive electron-donating effect than the *tert*-butyl moiety. The CO stretching frequencies for *trans*-L₂Rh(CO)Cl complexes followed the trend TTBP < DTBNpP < TBDNpP < TNpP, which was consistent with this expectation.^{16a} Calculated HOMO energy levels for the free ligands showed that the HOMO energy level of the free ligand increased going from TNpP to TTBP. In contrast, the HOMO energy levels for the LPd(0) complexes, which are the presumed catalytically active species, were similar for all four ligands.

On the basis of these results, DTBNpP appeared to have optimal steric and electronic properties for couplings of aryl bromides, whereas TBDNpP and TNpP were perhaps too large to form active catalysts. The lower activity of DTBNpP toward aryl chlorides was tentatively attributed to the lower electron-donating ability of DTBNpP compared to TTBP. Previous results from our laboratory and others have indicated that steric demand is the key factor in determining catalyst efficiency for couplings of aryl bromides.^{15b,16a,18} Since the C–Cl bond is stronger, more electron-rich palladium centers are required to activate aryl chlorides, resulting in a stronger dependence on electronic effects in coupling of aryl chlorides.

Although sterically demanding ligands provide high activity catalysts for unhindered substrates, these catalysts often show lower activity with sterically demanding substrates. For example, coupling of 2,6-disubstituted aryl halides with 2,6-disubstituted anilines is challenging for commonly used catalyst systems based on tri-*tert*-butylphosphine or S-phos.^{8,19} 2,6-Dimethyl-substituted aryl bromides and chlorides have been coupled with 2,6-disubstituted anilines (substituent = methyl, isopropyl) in good yields using preformed *N*-heterocyclic carbene palladium complexes,^{7d,20} diketimate palladium complexes,²¹ proazaphosphatane-derived catalysts,^{6b} and iminoproazaphosphatane-phosphine/Pd systems.²² Catalysts derived from simple phosphines generally afford low conversions or require high temperatures and/or high catalyst loadings with these more challenging substrates,^{16a,19,23} although Nolan has reported an effective palladium-allyl phosphine precatalyst for these couplings.²⁴ Rodriguez and Tang recently reported an oxaphosphole ligand that provides active catalysts for the coupling of bromo-2,4,6-triisopropyl-

benzene with 2,6-diisopropylaniline in good yield at 110 °C.⁸ There are few other examples of coupling similarly hindered substrates.^{7d,22}

Previously, our group compared the activity of catalysts derived from the neopentylphosphine series (Figure 1) in the Suzuki–Miyaura, Sonogashira, Heck, and Buchwald–Hartwig cross-coupling reactions.¹⁶ It was determined that DTBNpP provides the highest activity catalyst under mild conditions with unhindered substrates, whereas the catalysts derived from TBDNpP and TNpP afford lower activity. The DTBNpP/Pd catalyst system provides low conversions with sterically hindered substrates, however. Attempted coupling of 2-bromo-*m*-xylene with phenylboronic acid gave no conversion to product at room temperature or 80 °C.^{16b} A subsequent ligand screening for this reaction at 80 °C showed that the catalyst derived from TNpP and Pd(OAc)₂ gave an 87% yield of 2,6-dimethylbiphenyl (eq 1). Based on the calculated steric



parameters for these ligands, it was surprising that TNpP gave a more effective catalyst for coupling for hindered substrates than DTBNpP. We hypothesized that the increased conformational flexibility of TNpP compared to DTBNpP may allow it to better accommodate sterically hindered substrates in the coordination sphere.

Herein, we report the use of the conformationally flexible trineopentylphosphine (TNpP) ligand in the Buchwald–Hartwig amination and the Suzuki–Miyaura coupling of sterically congested substrates. A wide variety of aryl bromides and chlorides are coupled with mono- or di-*ortho*-substituted aryl amines and boronic acids. The reported catalyst system utilizes a simple, readily synthesized phosphine that can provide an active catalyst in situ with a suitable palladium precursor. In contrast to the air sensitivity of many simple trialkylphosphines, such as TTBP or DTBNpP, TNpP shows no degradation in air as a solid over a 9-day period or in solution over a period of 24 h.^{16b}

RESULTS

Amination of Aryl Bromides. Catalysts derived from DTBNpP and TNpP were compared in the coupling of a series of aryl bromides and aniline derivatives with increasing steric bulk (Table 1) to explore the tolerance of these catalysts for sterically hindered substrates. The coupling of 4-bromotoluene with 2,4,6-trimethylaniline was performed using 0.5 mol % of Pd₂(dba)₃ and either 1 mol % of DTBNpP or 1 mol % of TNpP at 80 °C in toluene for 2 h at 80 °C. Both catalyst systems gave high conversions of the product (Table 1, entry 1). Using the more sterically demanding 2,6-diisopropylaniline resulted in a significant decrease in the yield obtained using DTBNpP, whereas the TNpP-derived catalyst again gave a high yield of product (Table 1, entry 2). Using the more hindered 2-bromo-*m*-xylene substrate resulted in a further decrease in yield for the DTBNpP system in the coupling with 2,4,6-trimethylaniline, whereas the TNpP-derived catalyst was again unaffected by the increase in steric demand (Table 1, entry 3). The catalyst derived from DTBNpP gave almost no product in the coupling of 2-bromo-*m*-xylene with 2,6-diisopropylaniline.

Table 1. Comparison Study of DTBNpP and TNpP^a

entry	R ¹	R ²	R ³	R ⁴	product	PR ₃	yield (%) ^b
1	Me	H	Me	Me		DTBNpP	100
						TNpP	94
2	Me	H	<i>i</i> -Pr	H		DTBNpP	44
						TNpP	96
3	H	Me	Me	Me		DTBNpP	20
						TNpP	94
4	H	Me	<i>i</i> -Pr	H		DTBNpP	4
						TNpP	95

^aReaction conditions: aryl bromide (1.0 mmol), amine (1.2 mmol), Pd₂(dba)₃ (0.5 mol %), phosphine (1.0 mol %), NaO-*t*-Bu (1.5 mmol), toluene (2 mL), 80 °C, 2 h. ^bDetermined by GC.

In contrast, TNpP gave the desired product in 95% yield (Table 1, entry 4). These results show that the Pd/DTBNpP catalyst system is sensitive to steric bulk around both the aryl halide and amine substrate, while the catalyst derived from TNpP is unaffected by the steric demand in these substrates.

To further explore the effect of ligand structure on the coupling of hindered substrates, a range of phosphines were used in the coupling of 1-bromo-2,4,6-triisopropylbenzene with 2,6-diisopropylaniline (Table 2). The commonly used TTBP ligand gave 36% conversion after 1 h. As expected on the basis of the results in Table 1, the DTBNpP-derived catalyst system gave no conversion to the desired product. TBDNpP gave only a 4% conversion after 1 h. TNpP gave 100% conversion of the desired product even with these very hindered substrates. Based on these results, other phosphines ligands were explored in this reaction. The catalyst system using tricyclohexylphosphine (PCy₃) also gave a nearly quantitative conversion to the diaryl amine product. The less hindered *n*-Bu₃P gave poor conversion. A good conversion (83%) was obtained with *t*-Bu₂PMe. Triphenylphosphine also gave a moderately active catalyst, whereas the more hindered P(*o*-tol)₃ gave a low conversion to product. On the basis of these results, there is not a clear correlation between cone angle values and catalyst efficiency in this reaction.

Reaction Scope. With these pleasing results, the Pd/TNpP catalyst system was subjected to a variety of sterically demanding aryl bromides with a range of sterically hindered anilines, and the results are shown in Table 3. The coupling of 2-bromo-*m*-xylene and bromomesitylene with 2,6-dimethylaniline gave the tetra-*o*-methyl-substituted diaryl amines in high yields in 1 h (2a, 2b). Interestingly, when 2,6-diisopropylaniline was used as the coupling partner, complete conversion occurred with a shorter reaction time (2c, 2d). 4-Bromotoluene was

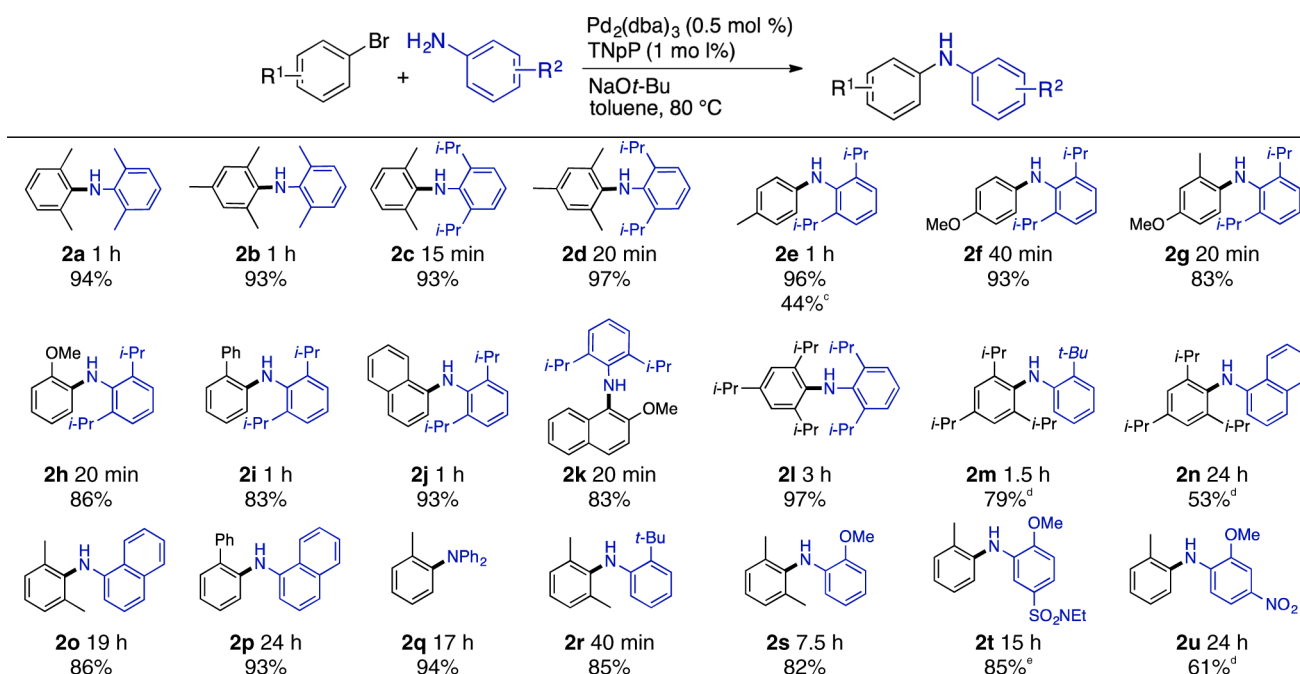
Table 2. Phosphine Screening in the Coupling of 1-Bromo-2,4,6-triisopropylbenzene and 2,6-Diisopropylaniline

entry	PR ₃	θ _{DFT} ^a (deg)	θ _T ^b (deg)	yield ^{c,d} (%)
1	TTBP	194	182	36
2	DTBNpP	198		0
3	TBDNpP	210		4
4	TNpP	227	180	100
5	PCy ₃		170	100
6	PBu ₃	177	132	3
7	<i>t</i> -Bu ₂ PMe			83
8	PPh ₃	173	145	76
9	P(<i>o</i> -tol) ₃	214 ^e	194	29

^aCone angle values determined from LDFT-optimized LPd(0) structures.^{16a} ^bCone angle values determined by Tolman.¹⁷ ^cReaction conditions: 1-bromo-2,4,6-triisopropylbenzene (1.0 mmol), 2,6-diisopropylaniline (1.2 mmol), Pd₂(dba)₃ (0.5 mol %), phosphine (1.0 mol %), NaO-*t*-Bu (1.5 mmol), toluene (2 mL), 80 °C, 1 h. ^dDetermined by GC analysis. ^eLiterature value.²⁵

coupled with 2,6-diisopropylaniline to obtain 96% of the desired product in 1 h (2e). Using DTBNpP in place of TNpP gave 2e in 44%, which is similar to that reported at room temperature using the Pd/DTBNpP catalyst system.^{16a} Electron-rich aryl bromides were coupled with 2,6-diisopropylaniline in high product yields with short reaction times (2f, 2g, 2h, 2k). Interestingly, the reaction time increased by a factor of 2 when there was no ortho substituent on the aryl bromide (2f) compared to an ortho methyl group being present (2g).

These conditions proved successful even with very sterically hindered substrates. For example, 1-bromo-2,4,6-triisopropylbenzene was coupled with 2,6-diisopropylaniline to give (2l) in 97% yield after 1 h. The increase in reaction time can be attributed to the steric hindrance of the bromide and amine. Coupling 1-bromo-2,4,6-triisopropylbenzene with 2-*tert*-butylaniline to give 2m required a higher catalyst loading (4 mol % Pd) for the reaction to reach completion. The extremely sterically hindered 2,4,6-tri-*tert*-butylaniline could not be coupled with any aryl bromide, including 4-bromotoluene. This result suggests either that the amine cannot coordinate to the palladium center or that reductive elimination is not possible due to the steric congestion around the amine. 1-Naphthylamine was coupled with 1-bromo-2,4,6-triisopropylbenzene using 2 mol % of Pd₂(dba)₃ and 4 mol % of TNpP with a moderate yield of 53% (2n). When 1-naphthylamine was coupled with other sterically hindered aryl bromides, high yields were obtained, although longer reaction times were required (2o, 2p). *o*-Anisidine was coupled with 2-bromo-*m*-xylene in 82% yield (2s). By placing electron-withdrawing groups on the aniline (such as sulfonamide or nitro groups), higher palladium loading and longer reaction times are needed (2t, 2u). In contrast to the successful formation of 2l using PCy₃ as the ligand, attempts to couple 1-bromo-2,4,6-

Table 3. Pd₂(dba)₃/TNpP-Catalyzed Coupling of Aryl Bromides^{a,b}

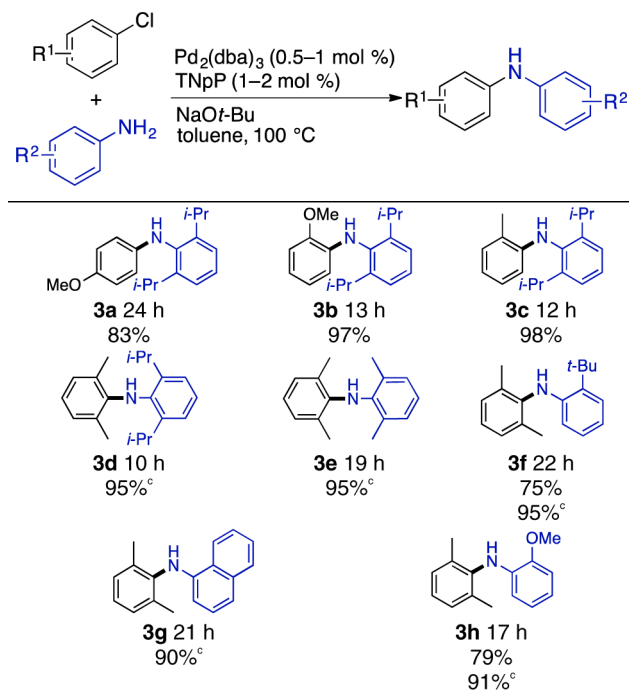
^aReaction conditions: aryl bromide (1.0 mmol), amine (1.2 mmol), Pd₂(dba)₃ (0.5 mol %), phosphine (1.0 mol %), NaO-*t*-Bu (1.5 mmol), toluene (2 mL), 80 °C. ^bIsolated yields (average of three runs). ^c1 mol % of DTBNpP used. ^dPd₂(dba)₃ (2 mol %), TNpP (4 mol %). ^ePd₂(dba)₃ (1 mol %), TNpP (2 mol %).

triisopropylbenzene with 2-*tert*-butylaniline or 1-naphthylamine to give **2m** and **2n**, respectively, with Pd₂(dba)₃ (2 mol %)/PCy₃ (4 mol %) gave low conversion to the desired product (<50%) and significant formation of 2,4,6-triisopropylbenzene.

Pd/TNpP-Catalyzed Amination of Aryl Chlorides.

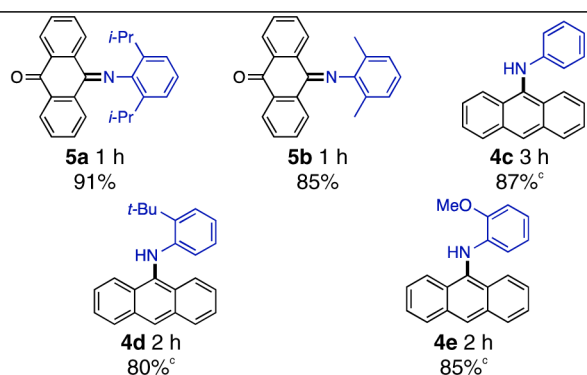
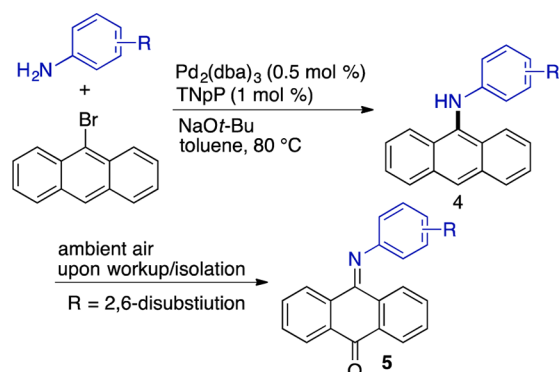
Good to excellent yields for aminations of sterically hindered aryl chlorides were obtained using the Pd₂(dba)₃/TNpP catalyst system. As was previously shown, higher temperature and higher catalyst loadings were needed to fully convert aryl chlorides to their desired products compared to aryl bromides.^{16a} Using the Pd₂(dba)₃/TNpP system, aryl chlorides with no or one *ortho*-substituent were coupled with 2,6-diisopropylaniline at 100 °C using 0.5 mol % of Pd₂(dba)₃ and 1.0 mol % of TNpP (Table 4). The electron-rich 4-chloroanisole and 2-chloroanisole gave 83% and 97%, respectively (**3a**, **3b**). As with aryl bromides, more sterically hindered substrates reacted faster than unhindered examples. 4-Chloroanisole required 24 h reach completion in the coupling with 2,6-diisopropylaniline, whereas only 12 and 13 h were required with 2-chloroanisole and 2-chlorotoluene, respectively. Di-*ortho*-substituted aryl chlorides, such as 2-chloro-*m*-xylene, required that the palladium loading be increased to 2 mol % to obtain high yields of the desired diaryl amine (**3d–h**), however. Tri-*ortho*-substituted products (**3f** and **3h**) were obtained in good yields with only 1 mol % of palladium. Increasing the palladium loading to 2 mol % allowed for complete conversions with yields above 90% for the coupled diaryl amines (**3f–h**), however.

TNpP/Pd₂(dba)₃ Coupling of 9-Bromoanthracene. To further explore the scope of the Pd₂(dba)₃/TNpP system, 9-bromoanthracene was coupled with 2,6-diisopropylaniline. Full conversion of 9-bromoanthracene occurred, but the isolated product was determined to be the anthraquinone monoimine (**5a**) rather than the expected 9-arylaminoanthracene. Oxidized

Table 4. TNpP/Pd₂(dba)₃-Catalyzed Coupling of Aryl Chlorides^{a,b}

^aReaction conditions: aryl chloride (1.0 mmol), amine (1.2 mmol), Pd₂(dba)₃ (0.5 mol %), phosphine (1.0 mol %), NaO-*t*-Bu (1.5 mmol), toluene (2 mL), 100 °C. ^bIsolated yields (average of three runs). ^cPd₂(dba)₃ (1 mol %), TNpP (2 mol %).

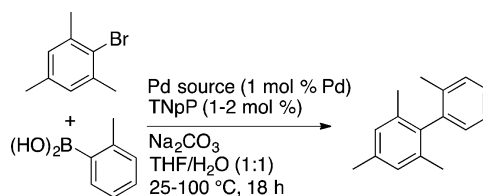
product **5a** was isolated in 91% yield (Table 5). The anthraquinone monoimine product was also isolated when 2,6-dimethylaniline was used as the coupling partner (**4b**). When aniline was used as the coupling partner, the 9-

Table 5. TNpP/Pd₂(dba)₃-Catalyzed Coupling of 9-Bromoanthracene^{a,b}

^aReaction conditions: 9-bromoanthracene (1.0 mmol), amine (1.2 mmol), Pd₂(dba)₃ (0.5 mol %), phosphine (1.0 mol %), NaO-*t*-Bu (1.5 mmol), toluene (2 mL), 80 °C. ^bIsolated yields (average of three runs). ^cPd₂(dba)₃ (1 mol %), TNpP (2 mol %).

phenylaminoanthracene product (**4c**) was obtained in 87% yield as the only product using 1 mol % of Pd₂(dba)₃. The 9-aminoanthracene products were also obtained with mono-*ortho*-substituted anilines (**4d** and **4e**) 9-Aminoanthracenes are known to undergo oxidation to the imine quinone form when treated with oxidants or, in some cases, upon air oxidation.²⁶ 9-Arylaminoanthracenes are typically stable in air, however, presumably because of delocalization of the amine lone pair into the aryl substituent. Based on this precedent, we hypothesized that compounds **5a** and **5b** formed by oxidation of the 9-arylaminoanthracene analogues. Treatment of aniline product **4c** under the reaction conditions for 24 h resulted in no oxidation, which suggested that the oxidation occurs upon exposure to air during workup. Next, the reaction of 9-bromoanthracene and 2,6-diisopropylaniline was performed under rigorously air-free conditions. The crude product was recovered without exposure to air and was shown to contain *N*-(2,6-diisopropylphenyl)-9-aminoanthracene (**4a**) and none of the monoimine anthraquinone form (**5a**) as determined by ¹³C NMR. Upon exposure to air, amines **4a** and **4b** underwent slow oxidation to give **5a** and **5b**. Complete oxidation occurred during purification by flash silica gel chromatography. The initial yellow amine product band turned to a bright red color as it was eluted. Therefore, amines **4a** and **4b** are formed under the coupling conditions followed by air oxidation to **5a** or **5b**. The increased air sensitivity of the hindered 9-aminoanthracenes (**4a** and **4b**) may be due to the decreased resonance delocalization of the nitrogen lone pair onto the aryl ring because the 2,6-disubstituted aryl substituent is forced to be roughly perpendicular to the 9-aminoanthracene unit.

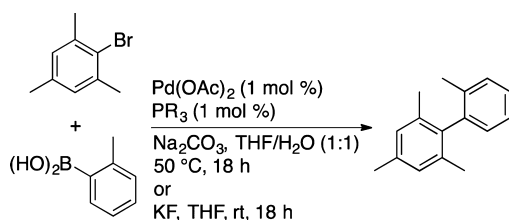
Suzuki–Miyaura Cross-Coupling. With the success of the TNpP system in the synthesis of hindered diarylamines, we focused our attention on the synthesis of hindered biaryls using the Suzuki coupling. Using TNpP as the ligand; the base, solvent, palladium source, and temperature were varied to obtain the optimal conditions for the Suzuki–Miyaura reaction. Both Pd(OAc)₂ (1 mol %) and Pd₂(dba)₃ (0.5 mol %) in combination with TNpP (1 mol %) gave comparable results in the reaction between bromomesitylene and *o*-tolylboronic acid in the presence of sodium carbonate in 1:1 THF/H₂O at 25 °C. Sodium carbonate was found to be the most efficient base when compared with cesium carbonate, cesium fluoride, and potassium fluoride. While previous publications by our group have indicated that TNpP requires elevated temperatures,^{16a} the coupling of bromomesitylene and *o*-tolylboronic acid gave moderate conversion at ambient temperature. Varying the temperature in reactions using catalysts formed from 1:1 and 1:2 Pd to ligand ratios with 1 mol % Pd indicated that 50 °C is the most effective temperature for this reaction with lower catalytic activity observed at higher and lower temperatures (Table 6).

Table 6. Optimization of the Palladium/TNpP-Catalyzed Suzuki–Miyaura Cross Coupling^a

palladium source	Pd:TNpP ratio	T (°C)	yield ^b (%)
Pd(OAc) ₂	1:1	25	64
		40	69
		50	84
	1:2	60	77
		80	69
		100	68
		25	67
		50	70
		80	56
Pd ₂ (dba) ₃	0.5:1	100	55
		25	71
		50	78
	0.5:2	80	56
		100	55
		25	60
		50	77
		60	72
		80	71
100	61		

^aReaction conditions: bromomesitylene (1.0 mmol), phenylboronic acid (1.1 mmol), palladium (1 mol %), TNpP (1–2 mol %) Na₂CO₃ (1.1 mmol) in water/THF (1:1, 2 mL). ^bYield determined by GC analysis.

With optimized conditions in hand for the Pd(OAc)₂/TNpP system, the series of neopentylphosphine ligands and TTBP were compared in the coupling of bromomesitylene and *o*-tolylboronic acid. The catalyst derived from TTBP gave a nearly quantitative yield (98%, Table 7). Among the neopentylphosphines, TNpP gave the highest conversion to

Table 7. Ligand Effect on the Coupling of Bromomesitylene and *o*-Tolylboronic Acid

entry	PR ₃	yield (%)	
		conditions A ^a	conditions B ^b
1	TTBP	98	98 (96) ²⁷
2	DTBNpP	14	7
3	TBDNpP	53	33
4	TNpP	68	42
5	PCy ₃	12	1

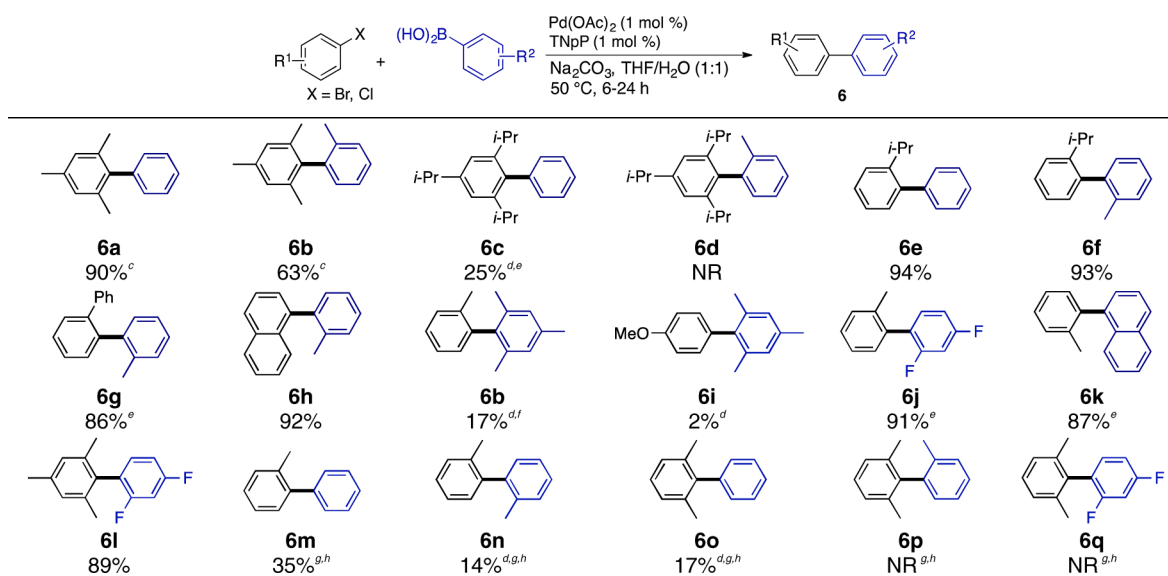
^aConditions A: bromomesitylene (1.0 mmol), 2-tolylboronic acid (1.1 mmol), Pd(OAc)₂ (1 mol %), TNpP (1 mol %), Na₂CO₃ (1.1 mmol) in water/THF (1:1, 2 mL) at 50 °C, 18 h. ^bConditions B: bromomesitylene (1.0 mmol), 2-tolylboronic acid (1.2 mmol, recrystallized from H₂O), Pd₂(dba)₃ (0.5 mol %), TNpP (1 mol %), KF (3.3 mmol), THF (2 mL), rt, 18 h.

product (68%). The catalyst derived from TBDNpP gave a lower conversion than the TNpP-derived catalysts, whereas DTBNpP and PCy₃ gave nearly inactive catalysts. The trend among the neopentylphosphines was the same as that seen in the amination reactions above. In contrast to the aminations, TTBP retained high conversion even with the hindered substrates, whereas PCy₃ gave an ineffective catalyst. The effectiveness of the ligands was also tested under anhydrous conditions reported by Fu and co-workers.²⁷ The trend was identical to that seen under the aqueous-biphasic conditions, but the yields obtained for the neopentylphosphines were lower under the anhydrous conditions. The TTBP-derived catalyst again gave a nearly quantitative yield of the biaryl product.

The optimized conditions were used for a range of substrates, shown in the Table 8. Moderately hindered aryl bromides were readily coupled with minimally hindered aryl boronic acids. Bromomesitylene gave good yields in couplings with phenylboronic acid (**6a**) and 2,4-difluorophenylboronic acid (**6l**). A lower yield was obtained when *o*-tolylboronic acid was used (**6b**). Good yields were obtained in the coupling of *o*-tolylboronic acid with 1-bromo-2-isopropylbenzene (**6f**), 2-bromobiphenyl (**6g**), and 1-bromonaphthalene (**6h**). The very hindered 1-bromo-2,4,6-triisopropylbenzene substrate gave low yields, even with phenylboronic acid. The Pd/TNpP catalyst was more sensitive to steric bulk on the boronic acid than on the aryl bromide (**6c**). Attempted synthesis of **6b** by coupling 2-bromotoluene and mesitylboronic acid gave only a 17% yield at 100 °C. The TNpP-derived catalyst appears to be particularly sensitive to sterically hindered boronic acid substrates in the transmetalation or reductive elimination steps.

Unlike the amination reaction, the Pd(OAc)₂/TNpP catalyst gave low conversions with aryl chlorides, even at elevated temperatures. Low yields of coupled products were obtained with 2-chlorotoluene and phenylboronic acid and *o*-tolylboronic acid (**6m** and **6n**). 2-Chloro-*m*-xylene and phenylboronic acid were coupled to give 17% conversion to **6o**. Attempts to couple this chloride with more hindered aryl boronic acids were unsuccessful, however. Given the success of TNpP in the amination of aryl chlorides, the lack of reactivity in the Suzuki–Miyaura coupling is somewhat surprising.

Mechanistic Considerations. To better understand the nature of the Pd/TNpP catalyst system, we focused our attention on the unusual rate trend seen with sterically congested aryl halides compared to unhindered aryl halides in the Buchwald–Hartwig amination. As previously mentioned, there is a noticeable time increase with less hindered aryl bromides. For example, 2-bromo-*m*-xylene is coupled with 2,6-diisopropylaniline approximately three times faster than is 4-bromotoluene (20 min compared to 1 h). To better understand

Table 8. TNpP/Pd(OAc)₂-Catalyzed Suzuki Coupling of Aryl Bromides and Chlorides^{a,b}

^aAryl bromide substrate unless noted. Reaction conditions: aryl bromide (1.0 mmol), arylboronic acid (1.1 mmol), Pd(OAc)₂ (1 mol %), TNpP (1 mol %), Na₂CO₃ (1.1 mmol) in water/THF (1:1) at 50 °C, 6–24 h. ^bIsolated yields (average of two runs). ^cRoom temperature. ^dEstimated GC yield. ^e2.0 mol % of Pd(OAc)₂ and 2.0 mol % of TNpP. ^f100 °C. ^g80 °C. ^hAryl chloride.

this unexpected reactivity trend, a more detailed rate comparison was performed.

As shown in Figure 2, the reaction between 2-bromo-*m*-xylene and 2,6-diisopropylaniline proceeded at a higher initial

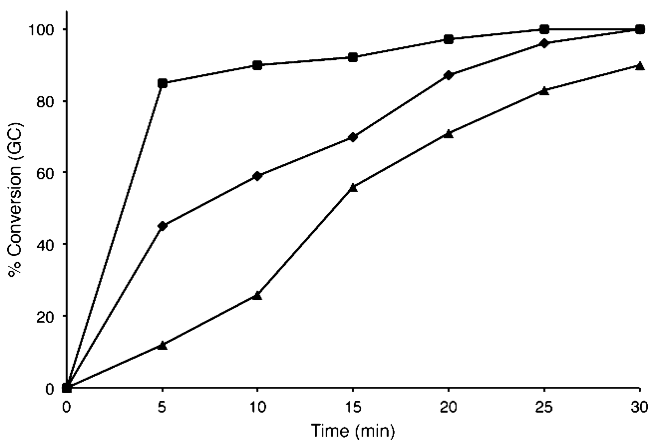
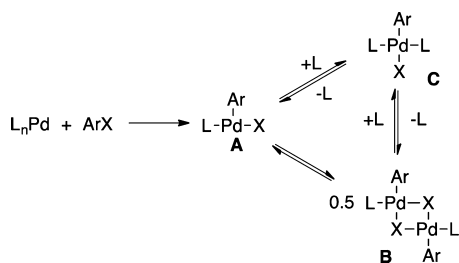


Figure 2. Conversion profiles for the TNpP/Pd(dba)₃-catalyzed (0.5 mol % of Pd, 1:1 L/Pd) coupling of aryl bromides with 2,6-diisopropylaniline at 80 °C: 2-bromo-*m*-xylene (square), 2-bromotoluene (diamond), and 1-bromo-4-*tert*-butylbenzene (triangle).

rate than that of 1-bromo-4-*tert*-butylbenzene. After 5 min, 85% of the 2-bromo-*m*-xylene had converted to the desired diaryl amine. In contrast, 1-bromo-4-*tert*-butylbenzene formed the desired product in only 12% conversion after 5 min. This reaction appears to show a slight induction period over the first 10 min, after which the reaction follows a normal reaction profile. The rate of formation of product from 2-bromotoluene was between that of 2-bromo-*m*-xylene and 1-bromo-4-*tert*-butylbenzene. These results are consistent with our previous observations in which sterically hindered substrates react at higher rate than sterically unhindered substrates.

Previous studies of oxidative addition of aryl halides to Pd/trialkylphosphine complexes have shown that the oxidative addition product formed depends on the steric properties of the ligand and aryl halide as well as the identity of the halide.²⁸ The possible oxidative addition products include 3-coordinated LPd(Ar)X complexes (A, Scheme 1), dimeric [LPd(Ar)X]₂

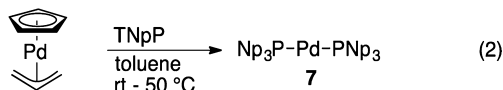
Scheme 1. Potential Oxidative Addition Products with Sterically Hindered Phosphine Ligands



complexes (B), and monomeric L₂Pd(Ar)X complexes (C). Type A complexes have been observed with very sterically demanding ligands, such as TTBP.²⁹ Dimeric complexes (B) are more commonly observed with hindered phosphine ligands.³⁰ Sterically undemanding ligands, such as triphenylphosphine or tricyclohexylphosphine, favor the bisphosphine products (C) when excess phosphine is present.³¹ We

considered that the steric effect on reaction rate might be due a difference in the equilibrium ratio of the possible oxidative addition products. To explore this hypothesis, the oxidative addition of hindered and unhindered aryl bromides to Pd(TNpP)₂ was studied.

Bis(trineopentylphosphine)palladium(0) (7) was prepared by reacting Pd(η⁵-Cp)(η³-allyl) with 2 equiv of TNpP (eq 2).³²



Recrystallization of 7 from toluene gave crystals suitable for structural characterization (Figure 3). Complex 7 crystallized in

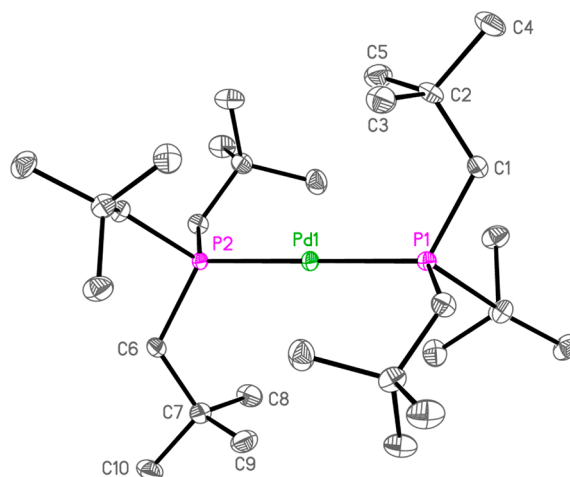


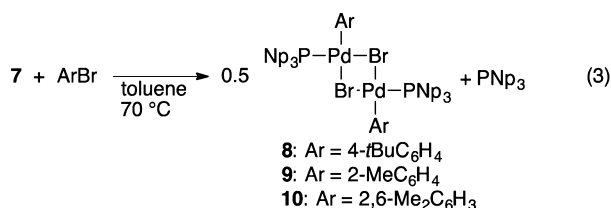
Figure 3. Thermal ellipsoid plot (50% probability) of the molecular structure of 7. Hydrogen atoms and disorder are omitted for clarity. Unlabeled atoms are symmetry equivalents of labeled atoms. Selected bond lengths (Å) and angles (deg): Pd–P1, 2.282(2); Pd–P2, 2.294(1); P1–Pd–P2, 180.00; Pd–P1–C1, 119.1(1); Pd–P2–C6, 118.5(1); P1–C1–C2, 119.5(2); P2–C6–C7, 121.2(2); C1–P1–C1', 98.3(1); C6–P2–C6', 99.1(1); Pd–P1–C1–C2, 34.2(3); Pd–P2–C6–C7, –34.9(3). Symmetry code for C1' and C6' = (1 + x – y, 1 – x, z).

space group P31c with 3-fold symmetry about the P–Pd–P axis, although the two TNpP moieties are not symmetrical with each other. The palladium and phosphorus atoms were found to be positionally disordered at a ratio of approximately 95 to 5. The minor P1–Pd–P2 fragment also resides on a crystallographic 3-fold axis, with the phosphorus atoms apparently bound to C4 and C10. However, the orientation of the neopentyl groups relative to the P1–Pd–P2 core is essentially the same, with the neopentyl groups oriented toward the Pd center.

The TNpP ligands adopt a staggered conformation looking down the P1–Pd–P2 axis. The Pd–P1 and Pd–P2 bond distances are 2.282(2) and 2.294(1) Å, respectively. The average Pd–P bond in 7 is shorter than the Pd–P distance in Pd(DTBNpP)₂ (2.2961(4) Å),^{16c} whereas the average Pd–P distance of 7 is similar to that reported for Pd(TTBP)₂ (2.285(3) Å).³³ The Pd–P1–C1–C2 dihedral angle is 34.2(3)°, and the Pd–P2–C6–C7 dihedral angle is –34.9(3)°. This conformation with a small Pd–P–C–C dihedral angle orients the steric bulk of the neopentyl group toward the metal center. The dihedral angle for complex 7 is larger than is seen in Pd(DTBNpP)₂ (0.3(1)°) due to the steric

strain between the neopentyl substituents on the two phosphine ligands. The neopentyl substituents have a moderate P1–C1–C2 angle of 119.5(2)° (P2–C6–C7 = 121.2(2)°), which is comparable to that seen in Pd(DTBNpP)₂ (119.62(9)°). The solid state structure is consistent with the previously calculated structure of **7**, which predicts that the neopentyl substituents project toward the Pd center exerting maximal steric influence.^{6a}

The oxidative addition of hindered and unhindered aryl bromides to bis(trineopentylphosphine)palladium(0) (**7**) was performed by reacting **7** with an excess of aryl bromide in toluene at 70 °C (eq 3).³⁴ The reaction mixture formed from **7**



and 1-bromo-4-*tert*-butylbenzene showed complete loss of **7** and new resonances for free TNpP (−57 ppm) and a new species at 7.7 ppm in a 1:1 ratio (Figure S1, Supporting Information). The pentane-insoluble material showed only the resonance at 7.7 ppm in its ³¹P NMR spectrum. The ¹H NMR spectrum of this material showed a 1:1 ratio of TNpP to the aryl group, suggesting the structure was of either type A or B.

Recrystallization of complex **8** from pentane gave X-ray quality crystals that upon crystallographic analysis showed the structure to be a dimeric type B structure (Figure 4). Complex **8** crystallized in the P2₁/c space group. The structure is consistent with dimeric structures of this type that have been

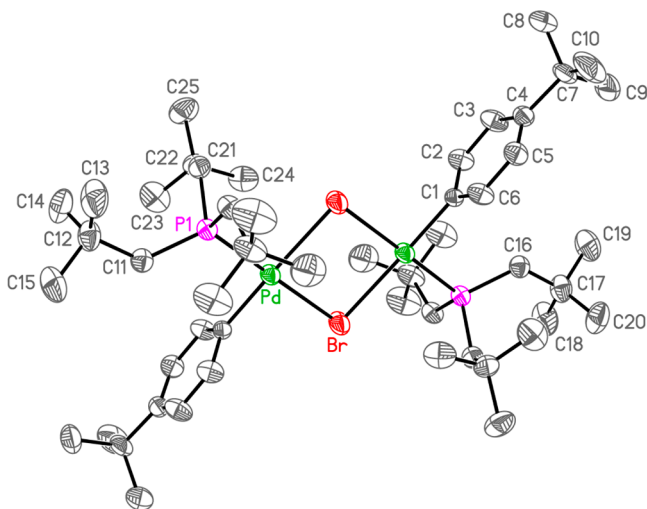
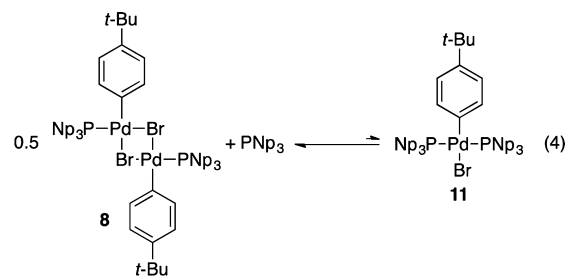


Figure 4. Thermal ellipsoid plot (50% probability) of the molecular structure **8**. Hydrogen atoms are omitted for clarity. Unlabeled atoms are symmetry equivalents of labeled atoms. Selected bond lengths (Å) and angles (deg): Pd–Br, 2.4992(7); Pd–Br', 2.5978(7); Pd–P, 2.245(1); Pd–C1, 2.003(5); Br–Pd–P, 177.27(4); Br'–Pd–P, 92.50(4); Br–Pd–C1, 89.8(1); Br'–Pd–C1, 174.5(1); Pd–Br–Pd', 93.44(2); Br–Pd–Br', 86.56(2); Pd–P1–C11, 118.4(2); Pd–P1–C16, 108.4(2); Pd–P1–C21, 111.1(2); P1–C11–C12, 127.5(4); P1–C16–C17, 121.9(4); P1–C21–C23, 113.3(5); Br–Pd–C1–C2, −83.9(4); Pd–P1–C11–C12, −179.9(4); Pd–P1–C16–C17, 55.8(4); Pd–P1–C21–C22, −81.8(4); C1–Pd–P1–C11, 6.9(2). Symmetry code for Br' and Pd' = (1 − x, 1 − y, 1 − z).

previously reported.³⁰ The Pd–C1 distance of 2.003(5) Å is similar to those of previously reported complexes, all of which have values near 2.00 ± 0.02 Å. The Pd–P distance for complex **8** (2.245(1) Å) falls between those of the PET₃ (2.2187(16) Å)³⁵ and P(*t*-Bu)₂Bu (2.2891(8) Å)^{30a} complexes reported in the literature.

The conformation of the trineopentylphosphine moiety is markedly different in complex **8** than in the Pd⁰ precursor **7**. In complex **7**, the ligands maintain a 3-fold symmetry with the neopentyl substituents directed in toward the palladium center resulting in small Pd–P–C–C dihedral angles. In complex **8**, the TNpP ligand adopts a C₁ conformation with each neopentyl substituent having a different Pd–P–C–C dihedral angle. Two of the neopentyl groups are located above and below the P₂Br₂ plane and have Pd–P–C–C dihedral angles of 55.8(4)° and −81.8(4)°, respectively. The third neopentyl group is in the P₂Br₂ plane approximately eclipsing the Pd–aryl bond (C1–Pd–P1–C11 = 6.9(2)°). In this case, the Pd–P–C–C dihedral angle is 179.9(4)°. The P–C–C angle in this neopentyl substituent is significantly larger (127.5(4)°) than for the other two neopentyl groups (111.1(2)° and 121.9(4)°), which suggests significant strain for the *anti*-oriented neopentyl group. The neopentyl substituents of complex **8** adopt a similar conformation to the ethyl substituents of [Pd(PET₃)(*p*-tol)Cl]₂.³⁵ Because of the smaller steric demand of the ethyl groups compared to the neopentyl substituents, the P–C–C angles are much smaller (112.0(5)°, 112.9(5)°, and 116.2(5)°), however.

The reaction of **7** with the aryl halide produces 0.5 equiv of **8** and 1 equiv of free TNpP. The ³¹P{¹H} NMR spectrum of the crude reaction mixture showed only complex **7** (7.74 ppm), a small peak at 6.3 ppm (<10% of **7**), and free TNpP (−57 ppm). Although the peak at 6.3 ppm has not been identified, it is likely a stereoisomer of **8** in which the aryl rings are *cis*-oriented. Similar *trans/cis* equilibria have been proposed to occur in solution for other [Pd(PR₃)(Ar)X]₂ complexes.³⁰ Notably, Pd(TNpP)₂(4-C₆H₄-*t*-Bu)Cl₂ (**11**) was not present in any significant amount. Thus, dimer **8** is strongly favored in the equilibrium with **11** even in the presence of a significant TNpP concentration (eq 4).



Analysis of the reaction mixture formed by heating 2-bromotoluene and complex **7** in C₆D₆ at 70 °C for 12 h by ³¹P NMR spectroscopy showed complete consumption of **7** and the formation of free TNpP and four new ³¹P NMR resonances at 7.45, 7.51, 8.57, and 8.66 ppm (1.1:1.0:4.0:5.1, Figure S2, Supporting Information). After separation from residual aryl halide and TNpP, the recovered material showed only the four resonances between 7 and 9 ppm in the same ratio as the reaction mixture. The ¹H NMR spectrum of this mixture gave a resolved set of 2-tolyl resonances and a very broad set of resonances for the neopentyl substituents. At 10 °C, neopentyl resonances were resolved to a single *tert*-butyl resonance and

two resonances for the methylene proton. The tolyl methyl group resolved into two peaks. The ^{31}P NMR spectrum of the sample in CD_2Cl_2 showed only two peaks at 8.45 and 8.54 ppm. Removing the solvent and redissolving this material in C_6D_6 gave the same pattern of four resonances to that originally observed in the crude mixture (Figure S2, Supporting Information). The ^1H NMR spectrum of **9** in CD_2Cl_2 at room temperature was similar to that seen with C_6D_6 with resolved tolyl resonances and a very broad set of neopentyl resonances. At -20°C , the neopentyl resonances resolved into multiple resonances with diastereotopic methylene units.

An X-ray quality crystal of complex **9** was obtained by recrystallization from diethyl ether. Structural analysis of this crystal showed a molecular structure (**9**, Figure 5) that is

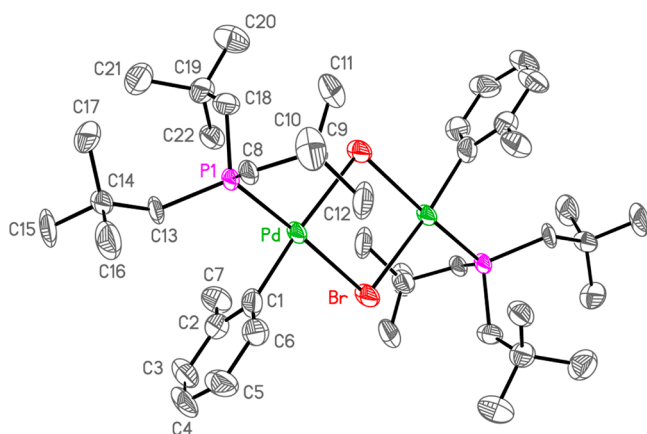


Figure 5. Thermal ellipsoid plot (50% probability) of the molecular structure of **9**. Hydrogen atoms are omitted for clarity. Unlabeled atoms are symmetry equivalents of labeled atoms. Selected bond lengths (Å) and angles (deg): Pd–Br, 2.504(2); Pd–Br', 2.573(2); Pd–P1, 2.266(3); Pd–C1, 2.00(2); Br–Pd–P1, 172.8(1); Br'–Pd–P1, 97.58(2); Br–Pd–C1, 87.1(4); Br'–Pd–C1, 173.8(5); Pd–Br–Pd', 93.13(6); Br–Pd–Br', 86.87(6); Pd–P1–C8, 110.7(4); Pd–P1–C13, 114.3(5); Pd–P1–C18, 114.4(5); P1–C8–C9, 124(1); P1–C13–C14, 128.7(9); P1–C18–C19, 122(1); Br–Pd–C1–C2, $-84(1)$; Pd–P1–C8–C9, 174(1); Pd–P1–C13–C14, 153(1); Pd–P1–C18–C19, $-71(1)$; C1–Pd–P1–C13, 30.0(6). Symmetry code for Br' and Pd' = $(1 - x, 2 - y, -z)$.

analogous to complex **8**. Both crystallized in the $P2_1/c$ space group and have similar structural parameters. Because of the perturbation of the *o*-methyl group, the TNpP ligand is rotated relative to the Pd_2Br_2 plane, and as a result, the large Pd–P–C–C dihedral angle is $153(1)^\circ$ rather than the $179.9(4)^\circ$ value seen in **8**. The other two dihedral angle values are qualitatively the same as found in **8**. The additional steric strain in this system is apparent in the increased P–C–C angles of the neopentyl groups ($122(1)^\circ$, $124(1)^\circ$, and $128.7(9)^\circ$) compared to complex **8** ($113.3(5)^\circ$, $121.9(4)^\circ$, $127.5(4)^\circ$).

In this structure, the methyl groups of the *o*-tolyl substituent are in an *anti* conformation and the two aromatic substituents are in a pseudo-*trans* orientation. We hypothesize that the other species observed by ^{31}P NMR spectroscopy represent stereoisomers of the structure seen in the solid state. The peaks at 8.57 and 8.66 ppm are due to structures **9** and **12** in which the aryl groups are pseudo-*trans* and the methyl substituents are either syn or anti (Figure 6). In solution, these isomers are observed in nearly equal amounts, whereas only the anti-isomer **9** was observed in the solid state structure. The minor peaks seen at 7.45 and 7.51 ppm may be due to structures **13** and **14**

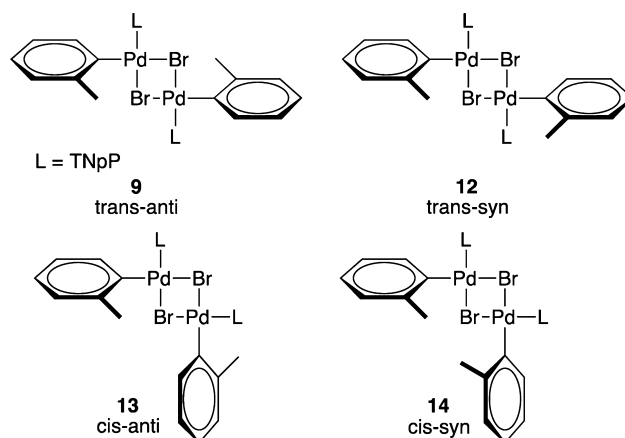


Figure 6. Stereoisomeric structures of complex **9**.

in which the aryl groups are pseudo-*cis* and the methyl groups can be either syn or anti. The *cis/trans* equilibrium was reported to be dependent on solvent polarity for the diadamantyl-*n*-butylphosphine analog of **9**.^{30a} The major/minor ratio increased from 3:1 to 9:1 upon changing the solvent from THF- d_8 to toluene- d_8 , which was rationalized as an increased preference for the *trans*-isomer in the less polar solvent. Complex **9** displays a similar solvent dependent equilibria, but in this case the major/minor ratio increases from approximately 5:1 in C_6D_6 to >20:1 for the major isomer in CDCl_3 . Assuming that the major isomer observed in solution is the *trans*-isomer obtained in the solid state (**9**), the solvent effect would appear to be opposite to that proposed by Beller.^{30a}

Reaction of 2-bromo-*m*-xylene with complex **7** did not result in the isolation of an oxidative addition complex (**10**) in analogy to complexes **8** and **9**. Instead, two peaks at 38 and 39 ppm in a 3.3:1 ratio along with free TNpP (38/39 ppm:TNpP = 1:1) were observed in the ^{31}P NMR spectrum of the reaction mixture. After the crude product was washed with pentane to remove excess 2-bromo-*m*-xylene and TNpP, a colorless powder (**15**) was obtained. The ^1H NMR spectrum of **15** shows no protons in the aromatic region. Thus, complex **15** is not an oxidative addition product. Repeating the reaction with bromomesitylene gave an identical ^{31}P NMR spectrum. Gas chromatographic analysis of the reaction mixture showed the formation of mesitylene. This result suggests the formation of an oxidative addition product that decomposes to give complex **15** and mesitylene.

During the course of the reaction of **7** with 2-bromo-*m*-xylene, an intermediate is observed at 8.5 ppm, which decays away as the starting material is consumed (Figure S3, Supporting Information). The intermediate observed at 8.5 ppm suggests that a dimeric complex similar to **8** and **9** is formed (**10**), but that this complex decomposes to give **15**. Because the species observed at 8.5 ppm decomposes as it is being formed, it could not be isolated and characterized. Complex **15** was observed in very small amounts in the oxidative addition of 1-bromo-4-*tert*-butylbenzene and 2-bromotoluene to complex **7**. The process to form **15** is apparently favored with the more sterically hindered *m*-xylyl and mesityl substituents, however. Attempts to obtain X-ray quality crystals of **15** have so far been unsuccessful.

DISCUSSION

Trineopentylphosphine provides a catalyst that is highly effective for the Buchwald–Hartwig amination of sterically hindered substrates. The Pd/TNpP catalyst system is one of the few systems reported to successfully couple a 2,6-diisopropyl-substituted aryl halide with a 2,6-diisopropylaniline derivative^{7,8,22} and the first example of arylation of 2-*tert*-butylaniline with a 2,6-disubstituted aryl halide. Although TNpP is calculated to have a very large cone angle based on the structure of Pd(TNpP), the catalyst derived from TNpP outperforms a range of other phosphine ligands, including those with smaller calculated cone angles.

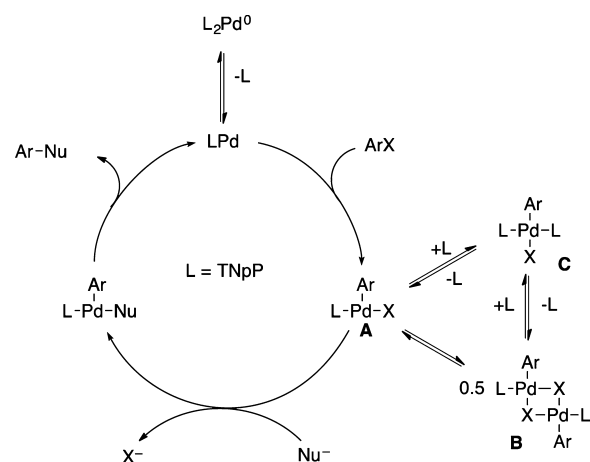
Based on solid-state structures obtained for complexes **7**, **8**, and **9**, the conformational flexibility of TNpP likely accounts for its ability to provide effective catalysts for these challenging coupling reactions. In the two-coordinate complex **7**, the neopentyl substituents adopt a conformation in which they are directed toward the palladium center. This conformation is similar to that obtained for the calculated gas-phase structure and predicts a large cone angle for TNpP coordinated to a low-coordination number metal. Complexes **8** and **9** show that the TNpP is able to adopt a less sterically demanding conformation in order to accommodate additional ligands at the metal center. This conformational flexibility may account for the particular effectiveness of the Pd/TNpP catalyst system with sterically hindered substrates. It is possible that the TNpP-derived catalyst has an effectively smaller steric demand that allows it to effectively react with sterically demanding substrates. Ligands with more rigid substituents, such as *tert*-butyl or cyclohexyl, are less able to accommodate these hindered substrates.

Interestingly, the Pd/TNpP catalyst system gives higher cross-coupling rates for sterically hindered aryl halides and amines than for less hindered substrates. Plenio has observed a slight increase in rate for 2-substituted aryl bromides in Sonogashira couplings catalyzed by Pd/P(*t*-Bu)_{*n*}Cy_{3-*n*} systems, but the more hindered 2,6-disubstituted aryl bromides were significantly less reactive.^{15f} In our case, we observe that the 2-bromo-*m*-xylene gives a higher rate than the 2-bromotoluene (Figure 2), which reacts faster than the 4-bromotoluene. Even if the flexibility of the TNpP ligand allows it to better accommodate sterically demanding substrates, we initially would have predicted that less hindered substrates would provide higher reaction rates. We hypothesize that this unusually reactivity trend has to do with the speciation of the oxidative addition intermediates as a function of ligand and substrate steric demand. The identity of the oxidative addition product could be expected to affect the rate of the overall catalytic cycle.

With sterically demanding ligands, the monophosphine complex (**A**) is believed to be the oxidative addition product that lies on the catalytic cycle (Scheme 2). Therefore, conditions that favor this structure would be expected to produce higher rates. Complexes **B** and **C** would represent catalyst resting states whose presence would slow down the overall catalytic process. We hypothesized that the unusual rate trends that we observed as a function of the substrate steric demand may be related to a difference in the oxidative addition product distribution formed with each aryl halide.

Initial study of the oxidative addition of aryl halides to Pd(TNpP)₂ shows that unhindered and 2-substituted aryl halides both form halide bridge dimer oxidative addition products (**B**). In solution, the dimeric complexes are resistant

Scheme 2. Mechanistic Pathway for Palladium-Catalyzed Coupling Reactions



to cleavage by TNpP to form Pd(TNpP)₂(Ar)Br (**C**). Therefore, **C**-type species likely do not play a role in the catalytic cycle with TNpP. Both 1-bromo-4-*tert*-butylbenzene and 2-bromotoluene gave the same oxidative addition products with qualitatively similar rates. Although we do not see a difference in the oxidative addition product formed, it is possible that the presence of the *ortho*-substituent would affect the equilibrium between **A** and **B**. Thus, with more hindered aryl halides, a higher equilibrium concentration of **A** would be present. In contrast, a sterically demanding, rigid ligand like TTBP gives stable 3-coordinate complexes independent of the steric demand of the aryl substituent.²⁹

Unfortunately, the oxidative addition product formed from Pd(TNpP)₂ and 2-bromo-*m*-xylene was unstable, so it was not possible to determine the structure of this product. Based on the chemical shift of the initially formed product, it is likely a dimeric structure similar to **8** and **9**. The low stability of this oxidative addition product does not appear to be relevant to the catalytic cycle given the high yields obtained with this and other 2,6-disubstituted aryl halides. Thus, in the presence of substrate, the oxidative addition product is sufficiently stable to continue on to product formation.

The identity of the decomposition products (**15**) is unknown, but there is prior precedent for similar decompositions of palladium aryl complexes with hindered ligands. The analogous [Pd(TTBP)(Ph)(μ -I)]₂ readily undergoes decomposition to biphenyl and [Pd(TTBP)(μ -I)]₂ upon heating.^{28a} Hartwig reported the formation of [Pd(TTBP)(μ -Br)]₂ and bithiophene when Pd(*dba*)₂, TTBP, and 2-bromothiophene were reacted together.³⁶ The [Pd(TTBP)(μ -Br)]₂ complex has also been seen as a byproduct in the oxidative addition of bromobenzene to Pd(TTBP)₂.³⁷

The observation of hydrodehalogenation products by GC in the oxidative addition of bromomesitylene to **7** is consistent with a similar decomposition pathway. The TNpP-derived materials (**15**) recovered from this reaction are not consistent with [Pd(TNpP)(μ -Br)]₂, however. Other known [Pd(PR₃)(μ -Br)]₂ complexes are intensely colored,³⁸ whereas the isolated material is a colorless solid. In addition, [Pd(PR₃)(μ -Br)]₂ complexes give ³¹P NMR shifts that are similar to those of the Pd(PR₃)₂ complexes, whereas the shifts we observe are significantly downfield of Pd(TNpP)₂, which is observed at -32 ppm. Finally, formation of [Pd(TNpP)(μ -Br)]₂ would not account for the appearance of two ³¹P NMR resonances that

appear to involve equilibrating species. The observed chemical shifts are inconsistent with other trineopentylphosphine derivatives that we have characterized, including trineopentylphosphine oxide (40 ppm), Pd(TNpP)₂Br₂ (25 ppm), [Pd(TNpP)(μ -Br)Br]₂ (0 ppm), Pd(TNpP)₂ (-32 ppm).

In the Suzuki coupling, TNpP provided a less effective catalyst than TTBP for the coupling of sterically demanding substrates, in contrast to the Buchwald–Hartwig amination. The increased steric demand of TTBP appears to be critical to the success of the Suzuki coupling based on our results (Table 7). This observation may reflect the need to maintain a higher equilibrium concentration of the 3-coordinate oxidative addition intermediate (A) relative to the halide bridged dimer (B). The TTBP ligand promotes formation of stable 3-coordinate oxidative addition products.²⁹ It is possible that the organoboron nucleophile is less effective in splitting the dimeric intermediate than more strongly coordinating amine substrates. Thus, the preference for the dimeric structure B may hinder the coupling reaction when TNpP is used as the ligand. It is noteworthy that TTBP is able to catalyze the Suzuki coupling of 2,6-disubstituted aryl bromides in contrast to DTBNpP, which provides an inactive catalyst. This result may suggest that DTBNpP has a larger effective steric demand than TTBP.

CONCLUSIONS

TNpP is a sterically demanding, electron-rich phosphine that effectively catalyzes the Hartwig–Buchwald amination of sterically hindered aryl bromides and chlorides with sterically demanding anilines. The TNpP-derived catalyst provides a significantly more effective catalyst with hindered substrates than TTBP. The TNpP-derived catalyst promoted amination of aryl chlorides occurs at lower temperature than was required by the DTBNpP-derived catalyst, even with unhindered aryl chlorides. The TNpP/Pd catalyst system catalyzes the Suzuki coupling of moderately hindered biaryl products, but is less effective with hindered substrates than TTBP. Structural analysis of TNpP complexes shows that TNpP adopts a large cone angle conformation when coordinated to a two-coordinate palladium but adopts a less hindered conformation when coordinated to a four-coordinate palladium center. This flexibility may account for trineopentylphosphine's unique ability to promote cross-coupling of high steric demand substrates. Notably, the TNpP-derived catalyst produces higher rates in the amination of sterically hindered aryl bromides than with unhindered aryl bromides. This unusual trend is hypothesized to be the result of a different equilibrium distribution of the oxidative addition products as a function of aryl halide steric demand. Further mechanistic studies to address this question are ongoing.

EXPERIMENTAL SECTION

General Experimental Details. All chemicals were obtained from commercial sources and used as received, except where noted. TNpP was obtained from FMC, Lithium Division. TNpP is stable in air for several days as a solid^{16b} but was stored in a nitrogen-filled glovebox. Pd(OAc)₂ and Pd₂(dba)₃ were provided by Johnson-Matthey. Toluene was distilled from sodium under nitrogen prior to use in coupling reactions. THF was distilled from sodium/benzophenone under nitrogen. Water was deoxygenated by sparging with nitrogen prior to use in Suzuki coupling reactions. All cross-coupling reactions were assembled in a nitrogen-filled glovebox. Reaction temperatures refer to previously equilibrated oil bath temperatures. ¹H and ¹³C NMR spectra are referenced to the NMR solvent peaks or internal TMS. ³¹P{¹H} NMR spectra were externally referenced to 85%

H₃PO₄. HRMS were obtained on a magnetic sector mass spectrometer using EI ionization and operating in the positive ion mode.

General Procedure for Buchwald–Hartwig Amination. A 10 mL screw-capped vial was placed in a glovebox where Pd₂(dba)₃ (0.5–2.0 mol %), TNpP (1.0–4.0 mol %), and NaO-*t*-Bu (1.5 equiv) were added. The vial was sealed with a rubber/Teflon septum and taken out of the glovebox. The aryl halide (1 mmol), arylamine (1.2 equiv), and 2 mL of toluene were added, and the reaction was placed in an oil bath preheated to 80 °C. After the reaction had reached completion as judged by GC, the reaction mixture was dissolved in ethyl acetate and filtered through a plug of silica gel. After drying, the crude reaction mixture was purified by flash chromatography on silica gel (0.5–10% EtOAc/hexane) to obtain pure product.

Bis(2,6-dimethylphenyl)amine (2a, 3e).^{6a} Using the general procedure, 2-bromo-*m*-xylene (133 μ L, 1.00 mmol) and 2,6-dimethylaniline (147 μ L, 1.20 mmol) were coupled using 0.5 mol % of Pd₂(dba)₃ and 1.0 mol % of TNpP at 80 °C to give the product as a white solid (211 mg, 94%). ¹H NMR (500 MHz, CDCl₃): δ 7.11 (d, *J* = 7.5 Hz, 4H), 6.97 (t, *J* = 7.5 Hz, 2H), 4.92 (s, 1H), 2.15 (s, 12H). ¹³C NMR (125 MHz, CDCl₃): δ 141.9, 129.7, 128.9, 121.9, 19.3.

Alternatively, 2-chloro-*m*-xylene (132 μ L, 1.00 mmol) and 2,6-dimethylaniline (147 μ L, 1.20 mmol) were coupled using 1.0 mol % of Pd₂(dba)₃ and 2.0 mol % of TNpP at 100 °C to obtain bis(2,6-dimethylphenyl)amine (214 mg, 95%).

***N*-(2,6-Dimethylphenyl)-2,4,6-trimethylaniline (2b).**^{6a} Using the general procedure, bromomesitylene (153 μ L, 1.00 mmol) and 2,6-dimethylaniline (147 μ L, 1.20 mmol) were coupled using 0.5 mol % of Pd₂(dba)₃ and 1.0 mol % of TNpP at 80 °C to give the product as a white solid (222 mg, 93%). ¹H NMR (500 MHz, CDCl₃): δ 7.14 (d, *J* = 7.4 Hz, 2H), 6.96–6.99 (m, 3H), 4.88 (s, 1H), 2.44 (s, 3H), 2.19 (s, 12H). ¹³C NMR (125 MHz, CDCl₃): δ 142.4, 139.2, 131.7, 130.7, 129.4, 128.9, 128.6, 121.2, 20.8, 19.3, 19.2.

***N*-(2,6-Dimethylphenyl)-2,6-diisopropylaniline (2c, 3d).**³⁹ Using the general procedure, 2-bromo-*m*-xylene (133 μ L, 1.00 mmol) and 2,6-diisopropylaniline (226 μ L, 1.20 mmol) were coupled using 0.5 mol % of Pd₂(dba)₃ and 1.0 mol % of TNpP at 80 °C to give the product as a clear, colorless oil (259 mg, 92%). ¹H NMR (500 MHz, CDCl₃): δ 7.19–7.23 (m, 3H), 7.03 (d, *J* = 7.4 Hz, 2H), 6.81 (t, *J* = 7.4 Hz, 1H), 4.89 (s, 1H), 3.25 (sept, *J* = 6.9 Hz, 2H), 2.08 (s, 6H), 1.22 (d, *J* = 6.9 Hz, 12H). ¹³C NMR (125 MHz, CDCl₃): δ 144.3, 143.3, 139.0, 129.7, 125.9, 125.0, 123.5, 119.8, 28.3, 23.7, 19.5.

Alternatively, 2-chloro-*m*-xylene (132 μ L, 1.00 mmol) and 2,6-diisopropylaniline (226 μ L, 1.20 mmol) were coupled using 1.0 mol % of Pd₂(dba)₃ and 2.0 mol % of TNpP at 100 °C to obtain *N*-(2,6-dimethylphenyl)-2,6-diisopropylaniline (267 mg, 95%).

***N*-(2,4,6-Trimethylphenyl)-2,6-diisopropylaniline (2d).**⁴⁰ Using the general procedure, bromomesitylene (153 μ L, 1.00 mmol) and 2,6-diisopropylaniline (226 μ L, 1.20 mmol) were coupled using 0.5 mol % of Pd₂(dba)₃ and 1.0 mol % of TNpP at 80 °C to give the product as a white solid (286 mg, 97%). ¹H NMR (500 MHz, CDCl₃): δ 7.21 (s, 3H), 6.86 (s, 2H), 4.81 (s, 1H), 3.24 (sept, *J* = 6.9 Hz, 2H), 2.33 (s, 3H), 2.07 (s, 6H), 1.23 (d, *J* = 6.9 Hz, 12H). ¹³C NMR (125 MHz, CDCl₃): δ 143.5, 140.7, 139.4, 130.3, 129.3, 126.5, 124.4, 123.4, 123.4, 28.2, 23.7, 20.6, 19.5.

***N*-(4-Methylphenyl)-2,6-diisopropylaniline (2e).**^{16a} Using the general procedure, 4-bromotoluene (123 μ L, 1.00 mmol) and 2,6-diisopropylaniline (226 μ L, 1.20 mmol) were coupled using 0.5 mol % of Pd₂(dba)₃ and 1.0 mol % of TNpP at 80 °C to give the product as a clear, colorless oil (257 mg, 96%). ¹H NMR (500 MHz, CDCl₃): δ 7.37–7.40 (m, 1H), 7.30–7.33 (m, 2H), 7.06 (d, *J* = 8.2 Hz, 2H), 6.52 (d, *J* = 8.3 Hz), 5.13 (s, 1H), 3.30 (sept, *J* = 6.9 Hz, 2H), 2.34 (s, 3H), 1.26 (d, *J* = 6.9 Hz, 12H). ¹³C NMR (125 MHz, CDCl₃): δ 147.6, 146.0, 135.8, 129.9, 127.2, 127.0, 124.0, 113.3, 28.4, 24.1, 20.6.

***N*-(4-Methoxyphenyl)-2,6-diisopropylaniline (2f, 3a).**^{16c} Using the general procedure, 4-bromoanisole (125 μ L, 1.0 mmol) and 2,6-diisopropylaniline (226 μ L, 1.20 mmol) were coupled using 0.5 mol % of Pd₂(dba)₃ and 1.0 mol % of TNpP at 80 °C to give the product as a clear, colorless oil (263 mg, 93%). ¹H NMR (500 MHz, CDCl₃): δ 7.37–7.40 (m, 1H), 7.33–7.34 (m, 2H), 6.86 (d, *J* = 9.0 Hz, 2H), 6.57 (d, *J* = 8.9 Hz, 2H), 5.11 (s, 1H), 3.83 (s, 3H), 3.34

(sept, $J = 6.8$ Hz, 2H), 1.27 (d, $J = 6.9$ Hz, 12H). ^{13}C NMR (125 MHz, CDCl_3): δ 152.4, 147.2, 142.4, 136.3, 126.9, 124.0, 114.9, 114.4, 55.8, 28.3, 24.0.

Alternatively, 4-chloroanisole (122 μL , 1.00 mmol) and 2,6-diisopropylaniline (226 μL , 1.20 mmol) were coupled using 0.5 mol % of $\text{Pd}_2(\text{dba})_3$ and 1.0 mol % of TNpP at 100 °C to obtain *N*-(4-methoxyphenyl)-2,6-diisopropylaniline (235 mg, 83%).

N-(4-Methoxy-2-methylphenyl)-2,6-diisopropylaniline (2g).

Using the general procedure, 4-bromo-3-methylanisole (141 μL , 1.00 mmol) and 2,6-diisopropylaniline (226 μL , 1.20 mmol) were coupled using 0.5 mol % of $\text{Pd}_2(\text{dba})_3$ and 1.0 mol % of TNpP at 80 °C to give the product as a red crystal (247 mg, 83%). ^1H NMR (500 MHz, CDCl_3): δ 7.31–7.34 (m, 1H), 7.27–7.29 (m, 2H), 6.82 (d, $J = 2.8$ Hz, 1H), 6.59 (dd, $J = 2.8$, $J = 8.7$ Hz, 1H), 6.13 (d, $J = 8.7$ Hz, 1H), 4.74 (s, 1H), 3.79 (s, 3H), 3.16 (sept, $J = 6.9$ Hz, 2H), 2.40 (s, 3H), 1.21 (br, 12H). ^{13}C NMR (125 MHz, CDCl_3): δ 152.2, 146.9, 140.4, 136.8, 126.2, 124.0, 123.5, 116.8, 113.0, 111.8, 55.8, 28.4, 24.9, 23.2, 18.1. HRMS m/z calcd for $\text{C}_{20}\text{H}_{27}\text{NO}$ (M^+) 297.2097, found 297.2090.

N-(2-Methoxyphenyl)-2,6-diisopropylaniline (2h, 3b).^{16c}

Using the general procedure, 2-bromoanisole (125 μL , 1.00 mmol) and 2,6-diisopropylaniline (226 μL , 1.20 mmol) were coupled using 0.5 mol % of $\text{Pd}_2(\text{dba})_3$ and 1.0 mol % of TNpP at 80 °C to give the product as a clear, colorless oil (244 mg, 86%). ^1H NMR (500 MHz, CDCl_3): δ 7.42–7.45 (m, 1H), 7.37–7.38 (m, 2H), 6.99 (dd, $J = 1.1$ Hz, $J = 7.6$ Hz, 1H), 6.80–6.89 (m, 2H), 6.29 (dd, $J = 1.6$ Hz, $J = 7.6$ Hz, 1H), 5.80 (s, 1H), 4.75 (s, 3H), 3.34 (sept, $J = 6.8$ Hz, 2H), 1.30 (d, $J = 6.9$ Hz, 12H). ^{13}C NMR (125 MHz, CDCl_3): δ 147.8, 146.2, 138.1, 135.6, 127.3, 123.9, 121.3, 117.0, 111.2, 110.0, 55.8, 28.4, 24.1.

Alternatively, 2-chloroanisole (127 μL , 1.00 mmol) and 2,6-diisopropylaniline (226 μL , 1.20 mmol) were coupled using 0.5 mol % of $\text{Pd}_2(\text{dba})_3$ and 1.0 mol % of TNpP at 100 °C to obtain *N*-(2-methoxyphenyl)-2,6-diisopropylaniline (274 mg, 97%).

***N*-(2-Biphenyl)-2,6-diisopropylaniline (2i).** Using the general procedure, 2-bromobiphenyl (172 μL , 1.00 mmol) and 2,6-diisopropylaniline (226 μL , 1.20 mmol) were coupled using 0.5 mol % of $\text{Pd}_2(\text{dba})_3$ and 1.0 mol % of TNpP at 80 °C to give the product as a white solid (273 mg, 83%). ^1H NMR (500 MHz, CDCl_3): δ 7.75 (d, $J = 7.4$ Hz, 2H), 7.65 (t, $J = 7.6$ Hz, 2H), 7.53 (t, $J = 7.4$ Hz, 1H), 7.42–7.45 (m, 1H), 7.33–7.38 (m, 3H), 7.23 (dt, $J = 1.0$ Hz, $J = 7.8$ Hz, 1H), 6.94 (t, $J = 7.4$ Hz, 1H), 6.41 (d, $J = 8.2$ Hz, 1H), 5.42 (s, 1H), 3.63 (sept, $J = 6.6$ Hz, 2H), 1.34 (d, $J = 6.9$ Hz, 6H), 1.25 (d, $J = 6.8$ Hz, 6H). ^{13}C NMR (125 MHz, CDCl_3): δ 147.6, 145.0, 139.7, 135.7, 130.3, 129.5, 129.2, 128.7, 127.6, 127.4, 127.2, 124.0, 117.6, 111.6, 28.6, 24.7, 23.1. HRMS: m/z calcd for $\text{C}_{24}\text{H}_{27}\text{N}$ (M^+) 329.2144, found 329.2147.

***N*-(2,6-Diisopropylphenyl)-1-naphthalenamine (2j).** Using the general procedure, 1-bromonaphthalene (207 mg, 1.00 mmol) and 2,6-diisopropylaniline (226 μL , 1.20 mmol) were coupled using 0.5 mol % of $\text{Pd}_2(\text{dba})_3$ and 1.0 mol % of TNpP at 80 °C to give the product as a white solid (282 mg, 93%). ^1H NMR (500 MHz, CDCl_3): δ 8.22–8.24 (m, 1H), 8.00–8.01 (m, 1H), 7.64–7.68 (m, 2H), 7.48–7.51 (m, 1H), 7.42–7.44 (m, 3H), 7.35 (t, $J = 7.8$ Hz, 1H), 6.37 (d, $J = 7.5$ Hz, 1H), 5.90 (s, 1H), 3.34 (sept, $J = 6.8$ Hz, 2H), 1.36 (d, $J = 6.9$ Hz, 6H), 1.27 (d, $J = 6.9$ Hz, 6H). ^{13}C NMR (125 MHz, CDCl_3): δ 147.2, 143.6, 135.8, 134.7, 129.0, 127.4, 126.8, 126.0, 125.2, 124.2, 123.5, 120.2, 118.3, 107.2, 28.4, 25.0, 23.4. HRMS: m/z calcd for $\text{C}_{22}\text{H}_{25}\text{N}$ (M^+) 303.1987, found 303.1982.

***N*-(2,6-Diisopropylphenyl)-2-methoxy-1-naphthalenamine (2k).** Using the general procedure, 1-bromo-2-methoxynaphthalene (237 mg, 1.00 mmol) and 2,6-diisopropylaniline (226 μL , 1.20 mmol) were coupled using 0.5 mol % of $\text{Pd}_2(\text{dba})_3$ and 1.0 mol % of TNpP at 80 °C to give the product as a colorless oil (290 mg, 83%). ^1H NMR (500 MHz, CDCl_3): δ 7.84 (d, $J = 8.1$ Hz, 1H), 7.56 (d, $J = 8.8$ Hz, 1H), 7.48 (d, $J = 8.8$ Hz, 1H), 7.40–7.43 (m, 2H), 7.32–7.36 (m, 3H), 7.15–7.18 (m, 1H), 6.12 (s, 1H), 4.07 (s, 3H), 3.51 (sept, $J = 6.8$ Hz, 2H), 1.33 (d, $J = 6.9$ Hz, 6H), 1.12 (d, $J = 6.9$ Hz, 6H). ^{13}C NMR (125 MHz, CDCl_3): δ 146.1, 143.7, 139.2, 131.5, 130.5, 128.4, 126.2, 125.0, 124.2, 123.8, 123.5, 123.1, 118.8, 113.7, 57.1, 28.3, 24.4, 22.9. HRMS: m/z calcd for $\text{C}_{23}\text{H}_{27}\text{NO}$ (M^+) 333.2093, found 333.2091.

N-(2,6-Diisopropylphenyl)-2,4,6-trisopropylaniline (2l).⁸

Using the general procedure, 1-bromo-2,4,6-trisopropylbenzene (253 μL , 1.00 mmol) and 2,6-diisopropylaniline (226 μL , 1.20 mmol) were coupled using 0.5 mol % of $\text{Pd}_2(\text{dba})_3$ and 1.0 mol % of TNpP at 80 °C to give the product as clear, colorless crystals (341 mg, 97%). ^1H NMR (500 MHz, CDCl_3): δ 7.27 (d, $J = 7.6$ Hz, 2H), 7.15–7.18 (m, 3H), 4.99 (s, 1H), 3.24–3.38 (m, 4H), 3.07 (sept, $J = 6.7$ Hz, 1H), 1.45 (dd, $J = 0.8$ Hz, $J = 6.9$ Hz, 6H), 1.92 (t, $J = 7.1$ Hz, 24H). ^{13}C NMR (125 MHz, CDCl_3): δ 143.8, 141.9, 141.2, 140.1, 138.3, 124.0, 122.3, 121.8, 34.2, 28.1, 27.9, 24.5, 23.9, 23.8.

***N*-(2-*tert*-Butylphenyl)-2,4,6-trisopropylaniline (2m).** Using the general procedure, 1-bromo-2,4,6-trisopropylbenzene (253 μL , 1.00 mmol) and 2-*tert*-butylaniline (187 μL , 1.20 mmol) were coupled using 2.0 mol % of $\text{Pd}_2(\text{dba})_3$ and 4.0 mol % of TNpP at 80 °C to give the product as a clear, colorless oil (278 mg, 79%). ^1H NMR (500 MHz, CDCl_3): δ 7.53 (d, $J = 7.8$ Hz), 7.31 (s, 2H), 7.15 (t, $J = 7.6$ Hz, 1H), 6.90 (t, $J = 7.6$ Hz, 1H), 6.43 (d, $J = 8.1$ Hz, 1H), 5.42 (s, 1H), 3.32 (sept, $J = 6.8$ Hz, 2H), 3.16 (sept, $J = 6.8$ Hz, 1H), 1.77 (s, 9H), 1.52 (d, $J = 6.9$ Hz, 6H), 1.40 (d, $J = 6.9$ Hz, 6H), 1.34 (d, $J = 6.9$ Hz, 6H). ^{13}C NMR (125 MHz, CDCl_3): δ 147.3, 146.9, 146.4, 133.7, 132.7, 127.2, 126.4, 122.0, 117.7, 113.6, 34.5, 34.4, 30.1, 28.6, 25.1, 24.4, 23.2. HRMS: m/z calcd for $\text{C}_{25}\text{H}_{37}\text{N}$ (M^+) 351.2926, found 351.2917.

***N*-(1-Naphthyl)-2,4,6-trisopropylaniline (2n).** Using the general procedure, 1-bromo-2,4,6-trisopropylbenzene (253 μL , 1.00 mmol) and 1-naphthylamine (172 mg, 1.20 mmol) were coupled using 2.0 mol % of $\text{Pd}_2(\text{dba})_3$ and 4.0 mol % of TNpP at 80 °C to give the product as a white solid (183 mg, 53%). ^1H NMR (500 MHz, CDCl_3): δ 8.13–8.15 (m, 1H), 7.93–7.95 (m, 1H), 7.58–7.63 (m, 2H), 7.33–7.35 (m, 1H), 7.27–7.30 (m, 1H), 7.21 (s, 2H), 6.30 (dd, $J = 0.9$ Hz, $J = 7.4$ Hz, 1H), 5.76 (s, 1H), 3.24 (sept, $J = 6.8$ Hz, 2H), 3.06 (sept, $J = 6.6$ Hz, 1H), 1.41 (d, $J = 6.9$ Hz, 6H), 1.28 (d, $J = 6.9$ Hz, 6H), 1.20 (d, $J = 6.9$ Hz, 6H). ^{13}C NMR (125 MHz, CDCl_3): δ 147.7, 146.9, 143.8, 134.7, 133.3, 129.1, 126.8, 126.0, 125.0, 123.3, 122.1, 120.2, 117.9, 106.9, 34.5, 28.5, 25.0, 24.4, 23.5. HRMS m/z calcd for $\text{C}_{25}\text{H}_{31}\text{N}$ (M^+) 345.2457, found 345.2469.

N-(2,6-Dimethylphenyl)-1-naphthalenamine (2o, 3g).⁴¹

Using the general procedure, 2-bromo-*m*-xylene (133 μL , 1.00 mmol) and 1-naphthylamine (172 mg, 1.20 mmol) were coupled using 0.5 mol % of $\text{Pd}_2(\text{dba})_3$ and 1.0 mol % of TNpP at 80 °C to give the product as a white solid (215 mg, 87%). ^1H NMR (500 MHz, CDCl_3): δ 8.20–8.22 (m, 1H), 8.00–8.01 (m, 1H), 7.64–7.68 (m, 2H), 7.47 (d, $J = 8.1$ Hz, 1H), 7.38 (d, $J = 8.0$ Hz, 1H), 7.33–7.35 (m, 2H), 7.27–7.30 (m, 1H), 6.43 (d, $J = 7.5$ Hz, 1H), 5.84 (s, 1H), 2.37 (s, 6H). ^{13}C NMR (125 MHz, CDCl_3): δ 141.4, 138.9, 135.4, 134.8, 128.9, 128.8, 126.7, 126.0, 125.7, 125.2, 124.2, 120.5, 119.0, 107.4, 18.3.

Alternatively, 2-chloro-*m*-xylene (132 μL , 1.00 mmol) and 1-naphthylamine (172 mg, 1.20 mmol) were coupled using 1.0 mol % of $\text{Pd}_2(\text{dba})_3$ and 2.0 mol % of TNpP at 100 °C to obtain *N*-(2,6-dimethylphenyl)-1-naphthalenamine (222 mg, 90%).

***N*-(2-Biphenyl)-1-naphthalenamine (2p).** Using the general procedure, 2-bromobiphenyl (172 μL , 1.00 mmol) and 1-naphthylamine (172 mg, 1.20 mmol) were coupled using 0.5 mol % of $\text{Pd}_2(\text{dba})_3$ and 1.0 mol % of TNpP at 80 °C to give the product as a white solid (274 mg, 93%). ^1H NMR (500 MHz, CDCl_3): δ 7.94 (t, $J = 10.8$ Hz, 2H), 7.67–7.68 (m, 3H), 7.44–7.56 (m, 7H), 7.40 (d, $J = 7.5$ Hz, 1H), 7.28 (t, $J = 7.6$ Hz, 1H), 7.18 (d, $J = 8.0$ Hz, 1H), 7.06–7.09 (m, 1H), 6.08 (s, 1H). ^{13}C NMR (125 MHz, CDCl_3): δ 142.1, 139.3, 139.2, 134.9, 130.9, 130.8, 129.5, 129.2, 128.7, 128.5, 128.4, 127.8, 126.3, 126.2, 125.9, 123.3, 122.1, 120.6, 117.1, 116.7. HRMS: m/z calcd for $\text{C}_{22}\text{H}_{17}\text{N}$ (M^+) 295.1361, found 295.1359.

***N*-(2-Tolyl)diphenylamine (2q).^{6b}** Using the general procedure, 2-bromotoluene (120 μL , 1.00 mmol) and diphenylamine (203 mg, 1.20 mmol) were coupled using 0.5 mol % of $\text{Pd}_2(\text{dba})_3$ and 1.0 mol % of TNpP at 80 °C to give the product as a white solid (251 mg, 97%). ^1H NMR (500 MHz, CDCl_3): δ 7.35–7.36 (m, 1H), 7.24–7.32 (m, 7H), 7.10 (dd, $J = 1.1$ Hz, $J = 8.7$ Hz, 4H), 7.03 (t, $J = 7.3$ Hz, 2H), 2.17 (s, 3H). ^{13}C NMR (125 MHz, CDCl_3): δ 147.7, 145.6, 136.7, 131.9, 129.8, 129.2, 127.5, 126.2, 121.7, 121.6, 18.8.

***N*-(2-*tert*-Butylphenyl)-2,6-dimethylaniline (2r, 3f).** Using the general procedure, 2-bromo-*m*-xylene (133 μ L, 1.00 mmol) and 2-*tert*-butylaniline (187 μ L, 1.20 mmol) were coupled using 0.5 mol % of Pd₂(dba)₃ and 1.0 mol % of TNpP at 80 °C to give the product as a white solid (215 mg, 85%). ¹H NMR (500 MHz, CDCl₃): δ 7.49 (dd, *J* = 1.4 Hz, *J* = 7.8 Hz, 1H), 7.27–7.29 (m, 2H), 7.20–7.23 (m, 1H), 7.09–7.12 (m, 1H), 6.91 (dt, *J* = 1.1 Hz, *J* = 8.2 Hz, 1H), 6.39 (dd, *J* = 1.1 Hz, *J* = 8.0 Hz), 5.49 (s, 1H), 2.34 (s, 6H), 1.72 (s, 9H). ¹³C NMR (125 MHz, CDCl₃): δ 144.1, 139.2, 135.3, 134.2, 128.8, 127.1, 126.6, 125.4, 118.7, 114.0, 34.7, 30.1, 18.8. HRMS: *m/z* calcd for C₁₈H₂₃N (M⁺) 253.1830, found 253.1837.

Alternatively, 2-chloro-*m*-xylene (132 μ L, 1.00 mmol) and 2-*tert*-butylaniline (187 μ L, 1.20 mmol) were coupled using 1.0 mol % of Pd₂(dba)₃ and 2.0 mol % of TNpP at 100 °C to obtain *N*-(2-*tert*-butylphenyl)-2,6-dimethylaniline (241 mg, 95%).

***N*-(2-Methoxyphenyl)-2,6-dimethylaniline (2s, 3h).**^{6b} Using the general procedure, 2-bromo-*m*-xylene (133 μ L, 1.00 mmol) and *o*-anisidine (135 μ L, 1.20 mmol) were coupled using 0.5 mol % of Pd₂(dba)₃ and 1.0 mol % of TNpP at 80 °C to give the product as a white solid (186 mg, 82%). ¹H NMR (500 MHz, CDCl₃): δ 7.22–7.23 (m, 2H), 7.16–7.19 (m, 1H), 6.96 (dd, *J* = 1.8 Hz, *J* = 7.4 Hz, 1H), 6.82 (dp, *J* = 1.7 Hz, *J* = 7.4 Hz, 2H), 6.25 (dd, *J* = 2.1 Hz, *J* = 7.5 Hz, 1H), 5.76 (s, 1H), 4.03 (s, 3H), 2.32 (s, 6H). ¹³C NMR (125 MHz, CDCl₃): δ 146.9, 138.6, 136.3, 136.2, 128.6, 125.9, 121.3, 117.4, 111.2, 110.0, 55.8, 18.4.

Alternatively, 2-chloro-*m*-xylene (132 μ L, 1.00 mmol) and *o*-anisidine (135 μ L, 1.20 mmol) were coupled using 1.0 mol % of Pd₂(dba)₃ and 2.0 mol % of TNpP at 100 °C to obtain *N*-(2-methoxyphenyl)-2,6-dimethylaniline (207 mg, 91%).

***N*-(2-Tolyl)-3-amino-*N,N*-diethyl-4-methoxybenzenesulfonamide (2t).** Using the general procedure, 2-bromotoluene (120 μ L, 1.00 mmol) and fast red ITR (310 mg, 1.20 mmol) were coupled using 1.0 mol % of Pd₂(dba)₃ and 2.0 mol % of TNpP at 80 °C to give the product as a yellow solid (293 mg, 85%). ¹H NMR (500 MHz, CDCl₃): δ 7.25–7.30 (m, 4H), 7.19 (t, *J* = 7.5 Hz, 1H), 7.04 (t, *J* = 7.4 Hz, 1H), 6.91 (d, *J* = 9.0 Hz, 1H), 6.01 (s, 1H), 3.97 (s, 3H), 3.19 (q, *J* = 7.2 Hz, 4H), 2.27 (s, 3H), 1.11 (t, *J* = 7.2 Hz, 6H). ¹³C NMR (125 MHz, CDCl₃): δ 150.3, 139.3, 135.0, 132.4, 131.2, 130.8, 126.9, 123.8, 121.3, 118.3, 110.8, 109.5, 56.0, 42.0, 17.8, 14.2. HRMS: *m/z* calcd for C₁₈H₂₄N₂O₃S (M⁺) 348.1508, found 348.1517.

***N*-(2-Tolyl)-2-methoxy-4-nitroaniline (2u).** Using the general procedure, 2-bromotoluene (120 μ L, 1.00 mmol) and 2-methoxy-4-nitroaniline (202 mg, 1.20 mmol) were coupled using 2.0 mol % of Pd₂(dba)₃ and 4.0 mol % of TNpP at 80 °C to give the product as a white solid (150 mg, 58%). ¹H NMR (500 MHz, CDCl₃): δ 7.82 (dd, *J* = 2.3 Hz, *J* = 8.9 Hz, 1H), 7.75 (d, *J* = 2.3 Hz, 1H), 7.32 (d, *J* = 8.5 Hz, 2H), 7.27 (t, *J* = 6.3 Hz, 1H), 7.19 (t, *J* = 7.4 Hz, 1H), 6.69 (d, *J* = 8.9 Hz, 1H), 6.53 (s, 1H), 4.04 (s, 3H), 2.28 (s, 3H). ¹³C NMR (125 MHz, CDCl₃): δ 145.8, 141.9, 138.6, 137.6, 133.2, 131.5, 127.2, 126.0, 124.7, 119.3, 109.2, 105.6, 56.3, 17.9. HRMS: *m/z* calcd for C₁₄H₁₄N₂O₃ (M⁺) 258.1004, found 258.1010.

***N*-(2-Tolyl)-2,6-diisopropylaniline (3c).**^{16c} Using the general procedure, 2-chlorotoluene (120 μ L, 1.00 mmol) and 2,6-diisopropylaniline (226 μ L, 1.20 mmol) were coupled using 0.5 mol % of Pd₂(dba)₃ and 1.0 mol % of TNpP at 100 °C to give the product as a clear, colorless oil (262 mg, 98%). ¹H NMR (500 MHz, CDCl₃): δ 7.47–7.50 (m, 1H), 7.41–7.43 (m, 2H), 7.31 (d, *J* = 7.3 Hz, 1H), 7.14 (t, *J* = 7.5 Hz, 1H), 6.86 (t, *J* = 7.3 Hz, 1H), 6.33 (d, *J* = 8.1 Hz, 1H), 5.10 (s, 1H), 3.33 (sept, *J* = 6.8 Hz, 2H), 2.53 (s, 3H), 1.38 (d, *J* = 6.7 Hz, 6H), 1.32 (d, *J* = 6.7 Hz, 6H). ¹³C NMR (125 MHz, CDCl₃): δ 147.4, 146.2, 135.9, 130.3, 127.3, 127.2, 124.0, 121.4, 117.7, 111.6, 28.4, 24.9, 23.2, 17.8.

10-(2,6-Diisopropylphenylimino)-9(10*H*)-anthracenone (5a). Using the general procedure, 9-bromoanthracene (257 mg, 1.00 mmol) and 2,6-diisopropylaniline (226 μ L, 1.20 mmol) were coupled using 0.5 mol % of Pd₂(dba)₃ and 1.0 mol % of TNpP at 80 °C to give the product as a red oil (334 mg, 91%). ¹H NMR (500 MHz, CDCl₃): δ 8.40 (d, *J* = 7.8 Hz, 2H), 8.01 (br, 2H), 7.63 (t, *J* = 7.4 Hz, 2H), 7.54 (br, 2H), 7.13–7.25 (m, 3H), 2.81 (sept, *J* = 6.8 Hz, 2H), 1.10 (d, *J* = 6.8 Hz, 12H). ¹³C NMR (125 MHz, CDCl₃): δ 183.8, 152.9, 147.5,

133.5, 133.2, 132.9, 131.2, 127.7, 127.5, 124.1, 123.9, 123.8, 29.1, 23.0. HRMS: *m/z* calcd for C₂₆H₂₅NO (M⁺) 367.1936, found 367.1947.

10-(2,6-Dimethylphenylimino)-9(10*H*)-anthracenone (5b). Using the general procedure, 9-bromoanthracene (257 mg, 1.00 mmol) and 2,6-dimethylaniline (147 μ L, 1.20 mmol) were coupled using 0.5 mol % of Pd₂(dba)₃ and 1.0 mol % of TNpP at 80 °C to give the product as a red solid (264 mg, 85%). ¹H NMR (500 MHz, CDCl₃): δ 8.37 (d, *J* = 7.8 Hz, 2H), 8.00 (br, 2H), 7.62 (t, *J* = 7.4 Hz, 2H), 7.53 (br, 2H), 7.12 (d, *J* = 7.5 Hz, 2H), 7.00 (t, *J* = 7.5 Hz, 1H), 2.02 (s, 6H). ¹³C NMR (125 MHz, CDCl₃): δ 183.7, 153.1, 149.4, 133.3, 132.6, 131.2, 128.7, 127.4, 127.0, 123.4, 123.3, 18.1. HRMS: *m/z* calcd for C₂₂H₁₇NO (M⁺) 311.1315, found 311.1310.

***N*-Phenyl-9-anthramine (4c).**⁴² Using the general procedure, 9-bromoanthracene (257 mg, 1.00 mmol) and aniline (109 μ L, 1.20 mmol) were coupled using 1.0 mol % of Pd₂(dba)₃ and 2.0 mol % of TNpP at 80 °C to give the product as a yellow solid (234 mg, 87%). ¹H NMR (500 MHz, CDCl₃): δ 8.24 (s, 1H), 8.21 (d, *J* = 7.7 Hz, 2H), 8.06 (d, *J* = 8.3 Hz, 2H), 7.44–7.51 (m, 4H), 7.16 (t, *J* = 7.5 Hz, 2H), 6.79 (t, *J* = 7.3 Hz, 1H), 6.60 (d, *J* = 7.7 Hz, 2H), 6.01 (br, 1H). ¹³C NMR (125 MHz, CDCl₃): δ 148.2, 132.7, 132.5, 129.5, 129.3, 129.0, 126.1, 125.7, 125.5, 124.1, 118.7, 114.1.

***N*-(2-*tert*-Butylphenyl)-9-anthramine (4d).** Using the general procedure, 9-bromoanthracene (257 mg, 1.00 mmol) and 2-*tert*-butylaniline (187 μ L, 1.20 mmol) were coupled using 1.0 mol % of Pd₂(dba)₃ and 2.0 mol % of TNpP at 80 °C to give the product as a yellow solid (260 mg, 80%). ¹H NMR (500 MHz, CDCl₃): δ 8.41 (s, 1H), 8.13 (d, *J* = 8.7 Hz, 2H), 8.06 (d, *J* = 8.4 Hz, 2H), 7.42–7.51 (m, 5H), 6.78–6.85 (m, 2H), 6.21 (s, 1H), 6.11 (dd, *J* = 1.6 Hz, *J* = 7.7 Hz, 1H), 1.79 (s, 9H). ¹³C NMR (125 MHz, CDCl₃): δ 146.2, 134.0, 133.6, 132.6, 129.0, 128.9, 127.3, 126.7, 126.1, 125.7, 124.9, 124.1, 118.9, 115.8, 34.9, 30.4. HRMS: *m/z* calcd for C₂₄H₂₃N (M⁺) 325.1830, found 325.1829.

***N*-(2-Methoxyphenyl)-9-anthramine (4e).** Using the general procedure, 9-bromoanthracene (257 mg, 1.00 mmol) and *o*-anisidine (135 μ L, 1.20 mmol) were coupled using 1.0 mol % of Pd₂(dba)₃ and 2.0 mol % of TNpP at 80 °C to give the product as an orange solid (254 mg, 85%). ¹H NMR (500 MHz, CDCl₃): δ 8.46 (s, 1H), 8.27 (d, *J* = 8.6 Hz, 2H), 8.11 (d, *J* = 8.2 Hz, 2H), 7.50–7.56 (m, 4H), 7.05 (d, *J* = 8.0 Hz, 1H), 6.83 (dt, *J* = 1.2 Hz, *J* = 7.6 Hz, 1H), 6.67–6.71 (m, 2H), 6.17 (dd, *J* = 1.2 Hz, *J* = 7.9 Hz, 1H), 4.16 (s, 3H). ¹³C NMR (125 MHz, CDCl₃): δ 146.7, 137.9, 113.2, 113.4, 129.3, 128.9, 126.0, 125.6, 125.3, 124.2, 121.3, 118.0, 112.3, 110.1, 55.9. HRMS: *m/z* calcd for C₂₁H₁₇NO (M⁺) 299.1310, found 299.1321.

General Procedure for the Suzuki–Miyaura Cross-Coupling. In a drybox, a 10 mL vial was charged with Pd(OAc)₂ (1–2 mol %), TNpP (1–2 mol %), arylboronic acid (1.10 mmol), Na₂CO₃ (1.10 mmol, 116 mg), and aryl halide (1.00 mmol). The vial was sealed with a septum cap, removed from the drybox, and charged with deoxygenated, dry THF (1 mL) and deoxygenated water (1 mL). The reaction mixture was allowed to stir in a 50 °C (or other temperature where noted) oil bath for 24 h or until determined to be complete by GC. Ethyl acetate (25 mL) was added to the reaction mixture, which was then washed with three 25 mL portions of brine. The organic layer was dried over MgSO₄ and the solvent was removed under reduced pressure. The crude products were purified by column chromatography through a short plug of silica gel using a gradient solution of hexane and ethyl acetate (0–10% EtOAc/hexanes) as the eluent.

2,4,6-Trimethylbiphenyl (6a).⁴³ Using the general procedure, bromomesitylene (153 μ L, 1.00 mmol) and phenylboronic acid (161 mg, 1.10 mmol) were coupled using 1 mol % of Pd(OAc)₂ and 1 mol % of TNpP at room temperature. The product was isolated as a yellow/clear oil (176 mg, 90%). ¹H NMR (500 MHz, CDCl₃): δ 7.32–7.20 (m, 3H), 7.04 (d, *J* = 7.5 Hz, 2H), 6.84 (s, 2H), 2.23 (s, 3H), 1.91 (s, 6H); ¹³C NMR (126 MHz, CDCl₃): δ 140.1, 138.0, 135.5, 134.5, 128.3, 127.3, 127.0, 125.5, 19.9, 19.7.

2,2',4,6-Tetramethylbiphenyl (6b, 6i).⁴⁴ Using the general procedure, bromomesitylene (153 μ L, 1.00 mmol) and 2-tolylboronic acid (149 mg, 1.10 mmol) were coupled using 1 mol % of Pd(OAc)₂ and 1 mol % of TNpP. The product was isolated as an orange oil (132

mg, 63%). ^1H NMR (500 MHz, CDCl_3): δ 7.39–7.32 (m, 3H), 7.13–7.11 (m, 1H), 7.05 (s, 2H), 2.45 (s, 3H), 2.03 (s, 6H); ^{13}C NMR (126 MHz, CDCl_3): δ 140.7, 138.3, 136.4, 135.8, 129.9, 129.3, 128.1, 127.0, 126.1, 21.2, 20.3, 19.5.

Alternatively, using the general procedure, 2-bromotoluene (85 mg, 0.50 mmol) and mesitylboronic acid (90 mg, 0.55 mmol) were coupled using 1 mol % of $\text{Pd}(\text{OAc})_2$, 1 mol % of TNpP, and 1.1 equiv of Na_2CO_3 (58 mg, 0.55 mmol). Gas chromatography was used to determine that the reaction had proceeded to 17% completion.

2,4,6-Triisopropylbiphenyl (6c). Using the general procedure, 1-bromo-2,4,6-triisopropylbenzene (245 μL , 1.00 mmol) and phenylboronic acid (161 mg, 1.10 mmol) were coupled using 2 mol % of $\text{Pd}(\text{OAc})_2$ and 2 mol % of TNpP. Gas chromatography was used to determine that the reaction had proceeded to 30% completion.

2-Isopropylbiphenyl (6e).⁴⁵ Using the general procedure, 1-bromo-2-isopropylbenzene (153 μL , 1.00 mmol) and phenylboronic acid (161 mg, 1.10 mmol) were coupled using 1 mol % of $\text{Pd}(\text{OAc})_2$ and 1 mol % of TNpP. The product was isolated as a colorless oil (184 mg, 94%). ^1H NMR (500 MHz, CDCl_3): δ 7.59–7.28 (m, 9H), 3.23 (sept, $J = 7.0$ Hz, 1H), 1.33 (d, $J = 6.7$ Hz, 6H); ^{13}C NMR (126 MHz, CDCl_3): δ 146.5, 142.3, 141.2, 130.1, 129.4, 128.1, 127.8, 126.8, 125.6, 125.4, 29.5, 24.4.

2-Isopropyl-2'-methylbiphenyl (6f).⁴⁶ Using the general procedure, 1-bromo-2-isopropylbenzene (153 μL , 1.00 mmol) and 2-tolylboronic acid (149 mg, 1.10 mmol) were coupled using 1 mol % of $\text{Pd}(\text{OAc})_2$ and 1 mol % of TNpP. The product was isolated as a colorless oil (192 mg, 93%). ^1H NMR (360 MHz, CDCl_3): δ 7.33–6.98 (m, 8H), 2.63 (sept, $J = 7.2$ Hz, 1H), 2.0 (s, 3H), 1.08 (d, $J = 7.2$ Hz, 3H), 1.01 (d, $J = 7.2$ Hz, 3H). ^{13}C NMR (126 MHz, CDCl_3): δ 146.8, 140.6, 136.2, 130, 129.9, 129.7, 127.9, 127.4, 125.6, 125.5, 30.1, 24.9, 23.5, 20.5.

2-Methyl-1,1',2',1''-terphenyl (6g). Using the general procedure, 2-bromobiphenyl (171 μL , 1.00 mmol) and 2-tolylboronic acid (149 mg, 1.10 mmol) were coupled using 2 mol % of $\text{Pd}(\text{OAc})_2$ and 2 mol % of TNpP. The product was isolated as an orange oil (204 mg, 86%). ^1H NMR (360 MHz, CDCl_3): δ 7.36–7.16 (m, 4H), 7.04–6.94 (m, 9H), 1.79 (s, 3H); ^{13}C NMR (126 MHz, CDCl_3): δ 141.5, 141.4, 141.1, 140.4, 135.9, 130.8, 130.7, 130.0, 129.9, 129.5, 127.9, 127.6, 127.2, 127.1, 126.5, 125.4, 20.2. HRMS m/z calcd for $\text{C}_{19}\text{H}_{16}$ (M^+) 244.1252, found 244.1246.

1-(2-Methylphenyl)naphthalene (6h, 6l).⁴⁷ Using the general procedure, 1-bromonaphthalene (140 μL , 1.00 mmol) and 2-tolylboronic acid (149 mg, 1.10 mmol) were coupled using 1 mol % of $\text{Pd}(\text{OAc})_2$ and 1 mol % of TNpP. The product was isolated as a white solid (201 mg, 92%). ^1H NMR (500 MHz, CDCl_3): δ 7.81 (dd, $J = 8.5, 18.9$ Hz, 2H), 7.46–7.17 (m, 9H), 1.95 (s, 3H); ^{13}C NMR (126 MHz, CDCl_3): δ 139.2, 138.8, 135.8, 132.51, 130.9, 129.3, 128.8, 127.2, 126.5, 125.4, 125.6, 125.1, 124.9, 124.7, 124.5, 124.3, 18.9. Mp: 66–67 °C (lit.⁴⁷ mp 65–66 °C).

Alternatively, using the general procedure, 2-bromotoluene (120 μL , 1.00 mmol) and 1-naphthaleneboronic acid (189 mg, 1.10 mmol) were coupled using 2 mol % of $\text{Pd}(\text{OAc})_2$ and 2 mol % of TNpP. The product was isolated as a white solid (190 mg, 87%).

2,4-Difluoro-2'-methylbiphenyl (6k). Using the general procedure, 2-bromotoluene (120 μL , 1.00 mmol) and 2,4-difluorophenylboronic acid (173 mg, 1.10 mmol) were coupled using 2 mol % of $\text{Pd}(\text{OAc})_2$ and 2 mol % of TNpP. The product was isolated as a colorless oil (188 mg, 91%). ^1H NMR (500 MHz, CDCl_3): δ 7.43–7.29 (m, 5H), 7.05–6.97 (m, 2H), 2.31 (s, 3H); ^{13}C NMR (126 MHz, CDCl_3): δ 162.5 (dd, $J = 11.3, 246.6$ Hz), 159.8 (dd, $J = 11.3, 246.6$ Hz), 136.8, 134.9, 132.2 (dd, $J = 5.4, 9.3$ Hz), 130.3, 130.1, 128.2, 125.8, 125.5 (dd, $J = 4.1, 17.1$ Hz), 111.2 (dd, $J = 5.3, 20.6$ Hz), 103.9 (dd, $J = 1.0, 26.4$ Hz), 19.90 (d, $J = 3.5$ Hz). HRMS-EI: m/z [M^+] calcd for $\text{C}_{13}\text{H}_{10}\text{F}_2$ 204.0751, found 204.0743.

2,4-Difluoro-2',4',6'-trimethylbiphenyl (6m). Using the general procedure, bromomesitylene (153 μL , 1.00 mmol) and 2,4-difluorophenylboronic acid (173 mg, 1.10 mmol) were coupled using 1 mol % of $\text{Pd}(\text{OAc})_2$ and 1 mol % of TNpP. The product was isolated as a colorless oil (206 mg, 89%). ^1H NMR (500 MHz, CDCl_3): δ 7.28–7.21 (m, 1H), 7.12 (s, 2H), 7.10–7.02 (m, 2H), 2.48 (s, 3H),

2.18 (s, 6H); ^{13}C NMR (126 MHz, CDCl_3): δ 162.4 (dd, $J = 11.8, 246.9$ Hz), 159.7 (dd, $J = 11.8, 246.9$ Hz), 137.7, 131.6, 128.4, 124.2 (dd, $J = 3.9, 19.5$ Hz), 111.4 (dd, $J = 3.8, 21.0$ Hz), 104.1 (q, $J = 1.0, 25.4$ Hz), 21.1, 20.4. HRMS-EI (m/z): [M^+] calcd for $\text{C}_{15}\text{H}_{14}\text{F}_2$ 232.1064, found 232.1061.

2-Methylbiphenyl (6n).⁴⁸ Using the general procedure, 2-chlorotoluene (117 μL , 1.00 mmol) and phenylboronic acid (161 mg, 1.10 mmol) were coupled at 80 °C using 1 mol % of $\text{Pd}(\text{OAc})_2$ and 1 mol % of TNpP. The product was isolated as a colorless oil (59 mg, 35%). ^1H NMR (500 MHz, CDCl_3): δ 7.50–7.47 (m, 2H), 7.42–7.39 (m, 3H), 7.35–7.28 (m, 4H), 2.35 (s, 3H); ^{13}C NMR (126 MHz, CDCl_3): δ 142.0, 141.9, 135.4, 130.3, 129.8, 129.2, 128.1, 127.3, 126.8, 125.8, 20.5.

2,2'-Dimethylbiphenyl (6o). Using the general procedure, 2-chlorotoluene (117 μL , 1.00 mmol) and 2-tolylboronic acid (149 mg, 1.10 mmol) were coupled using 1 mol % of $\text{Pd}(\text{OAc})_2$ and 1 mol % of TNpP. Gas chromatography was used to determine that the reaction had proceeded to 14% completion.

2,6-Dimethylbiphenyl (6p). Using the general procedure, 2-chloro-*m*-xylene (133 μL , 1.00 mmol) and phenylboronic acid (161 mg, 1.10 mmol) were coupled at 80 °C. Gas chromatography was used to determine that the reaction had proceeded to 17% completion.

Synthesis of bis(trineopentylphosphine)palladium(0) (7). In a glovebox, allyl(cyclopentadiene)palladium(II)²⁵ (200 mg, 0.94 mmol) and trineopentylphosphine (505 mg, 2.07 mmol) were added to a 25 mL round-bottom flask, which was capped with a 14/20 septum and placed on a Schlenk line. Toluene (10 mL) was added to the solids, and the solution was stirred at room temperature for 12 h and then heated to 50 °C and stirred overnight. After stirring, a gray precipitate formed and the solid was filtered under an inert atmosphere. The resulting solid was washed with pentane to remove any excess phosphine to obtain 7 as a gray solid (477 mg, 85%). ^1H NMR (500 MHz, C_6D_6): δ 1.47 (t, $J = 3.0$ Hz, 12 H), 1.35 (s, 54 H). ^{13}C NMR (500 MHz, C_6D_6): δ 49.4 (t, $J_{\text{C-P}} = 8.8$ Hz), 32.2 (t, $J_{\text{C-P}} = 3.9$ Hz), 31.8 (t, $J_{\text{C-P}} = 2.3$ Hz). $^{31}\text{P}\{^1\text{H}\}$ (202.5 MHz, C_6D_6): δ 31.7 (s).

General Procedure for the Synthesis of the Oxidative Addition Products. In a glovebox, 1 equiv of 7 was added to a 50 mL round-bottom flask, which was placed onto a Schlenk line and suspended in 10 mL of toluene, 5 equiv of the aryl bromide was added, and the reaction mixture was heated to 70 °C until 7 was fully consumed. The reaction mixture was dried, and pentane was added to precipitate the oxidative addition products.

[Pd(TNpP)(4-tert-butylphenyl)(μ -Br)]₂ (8). Using the general procedure, 7 (100 mg, 0.17 mmol) was reacted with 1-bromo-4-tert-butylbenzene (146 μL , 0.84 mmol) to give a white solid (89 mg, 94%). Crystals suitable for X-ray analysis were obtained from a concentrated solution of pentane cooled to 0 °C. ^1H NMR (500 MHz, C_6D_6): δ 7.63 (brd, $J = 5.9$ Hz, 2H), 7.10 (brd, $J = 7.5$ Hz, 2H), (brd, $J_{\text{P-H}} = 10.1$ Hz, 6H), 1.26 (brs, 27H), 1.23 (s, 9H). ^{13}C NMR (500 MHz, C_6D_6): δ 146.1, 135.5, 125.4, 40.1 (m), 34.4, 33.8 (m), 32.9 (d, $J_{\text{C-P}} = 3.1$ Hz), 32.1. $^{31}\text{P}\{^1\text{H}\}$ (202.5 MHz, C_6D_6): δ 7.7 (s).

[Pd(P(Np)₃)(*o*-tolyl)(Br)]₂ (9). Using the general procedure, 7 (100 mg, 0.17 mmol) was reacted with 2-bromotoluene (101 μL , 0.84 mmol) to give a white solid (78 mg, 89%). Crystals suitable for X-ray analysis were obtained from a concentrated solution of diethyl ether cooled to 0 °C. ^1H NMR (500 MHz, C_6D_6 , 298 K): δ 7.70 (brs, 1H), 7.02 (brs, 1H), 6.91 (brm, 2H), 3.00 (s, 3H), 0.6–2.1 (vbm, 33H); (500 MHz, C_6D_6 , 283 K): δ 7.63 (brs, 1H), 6.96 (brs, 1H), 6.85 (brm, 2H), 2.96, 2.93 (s, isomers, 3H), 2.96 (brs, 3H), 1.69–1.74 (m, 3H), 1.22 (brs, 27); (500 MHz, CD_2Cl_2 , 298 K): δ 7.34 (brs, 1H), 6.92 (brs, 1H), 6.81 (brm, 2H), 2.71, 2.68 (s, isomers, 3H), 1.72 (vbrs, 6H), 1.25 (vbrs, 27H); (500 MHz, CD_2Cl_2 , 253 K): δ 7.2–7.31 (m, 1H), 6.91 (brd, $J = 6.6$ Hz, 1H), 6.76–6.81 (m, 2H), 2.66, 2.63 (s, isomers, 3H), 2.33–2.41 (m, 1H), 2.00–2.04 (m, 1H), 1.76–1.85 (m, 2H), 1.47, 1.42, 1.32, 1.28 (s, 18 H), 0.86–0.93 (m, 1H), 0.73 (s, 9H), one P-CH₂ proton overlaps with the peaks at 1.28–1.47. $^{31}\text{P}\{^1\text{H}\}$ (202.5 MHz, C_6D_6): δ 7.45, 7.51, 8.57, and 8.66 ppm (1.1:1.0:4.0:5.1), mixture of stereoisomers; (202.5 MHz, CD_2Cl_2): δ 8.55, 8.62 (1:1.5), mixture of stereoisomers.

Reaction of 7 and 2-Bromo-*m*-xylene (11). Using the general procedure, 7 (100 mg, 0.17 mmol) was reacted with 2-bromo-*m*-xylene (112 μ L, 0.84 mmol) to give a white solid (yield not determined due to inability to characterize the final product). $^{31}\text{P}\{^1\text{H}\}$: (202.5 MHz, C_6D_6): δ , 38.8 (s), 37.9 (s) (1:2.3) ppm.

X-ray Crystallographic Data. X-ray crystallographic data collection was performed at 173.0(1) K using a Bruker diffractometer with a Platform 3-circle goniometer and an Apex 2 CCD area detector. Crystals were cooled under a cold nitrogen stream using an N-Helix cryostat. A hemisphere of data was collected for each crystal using a strategy of omega scans with 0.5° frame widths. Unit cell determination, data integration, absorption correction, and scaling were performed using the Apex2 software suite from Bruker.⁴⁹ Space group determination, structure solution, refinement, and generation of ORTEP diagrams were done using the SHELXTL software package.⁵⁰

The crystal structures of 7–9 were solved by direct methods and refined by full-matrix least-squares refinement against F^2 . Non-hydrogen atoms were located from the difference map and allowed to refine anisotropically. Hydrogen atoms were placed in calculated positions and refined using a riding model.

During the refinement of 7, three difference map peaks consistently appeared on an adjacent crystallographic 3-fold axis parallel to P1, Pd, and P2 after all expected atoms had been assigned and the refinement had converged. Certain carbon atoms also showed oblate thermal ellipsoids. Based on their position, it was realized that the difference map peaks could indicate positional disorder of the P1–Pd–P2 core across two separate 3-fold axes. To model this disorder, the occupancies of corresponding atoms were allowed to refine while the anisotropic displacement parameters of the atoms in the minor part were constrained to be equal to those of the corresponding atom in the major part. With this model, the site occupancies refined to a ratio of approximately 95:5. The atomic positions of the major part were not greatly affected, but the thermal ellipsoids improved while the R-factor decreased from 0.0563 to 0.0395. Because the site occupancy of the minor part was so small, carbon atoms or hydrogen atoms belonging to the minor part were not modeled.

■ ASSOCIATED CONTENT

■ Supporting Information

^1H and ^{13}C NMR spectra for coupling products in Tables 3–5 and 8; ^1H , ^{13}C , and ^{31}P NMR spectra of palladium complexes; and crystallographic information files for compounds 7–9 (CIF). This material is available free of charge via the Internet at <http://pubs.acs.org>.

■ AUTHOR INFORMATION

Corresponding Author

*E-mail: kshaughn@as.ua.edu.

Notes

The authors declare no competing financial interest.

■ ACKNOWLEDGMENTS

We thank the National Science Foundation (CHE-1058984) for financial support of this work, FMC, Lithium Division for donation of TNpP, and Johnson-Matthey for donation of palladium compounds. T.M.L. thanks the DAAD-RISE program.

■ REFERENCES

(1) (a) Budarin, V. L.; Shuttleworth, P. S.; Clark, J. H.; Luque, R. *Curr. Org. Synth.* **2010**, *7*, 614–627. (b) Johansson Seechurn, C. C. C.; Kitching, M. O.; Colacot, T. J.; Snieckus, V. *Angew. Chem., Int. Ed.* **2012**, *51*, 5062–5085. (c) *Palladium-Catalyzed Coupling Reactions*; Molnár, Á., Ed.; Wiley-VCH: Weinheim, 2013. (d) Nicolau, K. C.; Bulger, P. G.; Sarlah, D. *Angew. Chem., Int. Ed.* **2005**, *44*, 4442–4489.

(e) Torborg, C.; Beller, M. *Adv. Synth. Catal.* **2009**, *351*, 3027–3043. (f) Magano, J.; Dunetz, J. *Chem. Rev.* **2011**, *111*, 2177–2250.

(2) (a) Blaser, H.-U.; Indolese, A. F.; Naud, F.; Nettekoven, U.; Schnyder, A. *Adv. Synth. Catal.* **2004**, *346*, 1583–1598. (b) Hartwig, J. F. *Acc. Chem. Res.* **2008**, *41*, 1534–1544. (c) Surry, D. S.; Buchwald, S. L. *Angew. Chem., Int. Ed.* **2008**, *47*, 6338–6361. (d) Surry, D. S.; Buchwald, S. L. *Chem. Sci.* **2011**, *2*, 27–50.

(3) Carey, F. A.; Sundberg, R. J. *Advanced Organic Chemistry*, 5th ed.; Springer: New York, 2007.

(4) (a) Evano, G.; Blanchard, N.; Toumi, M. *Chem. Rev.* **2008**, *108*, 3054–3131. (b) Ma, D.; Cai, Q. *Acc. Chem. Res.* **2008**, *41*, 1450–1460. (c) Sorokin, V. I. *Mini-Rev. Org. Chem.* **2008**, *5*, 323–330. (d) Monnier, F.; Taillefer, M. *Angew. Chem., Int. Ed.* **2009**, *48*, 6954–6971. (e) Surry, D. S.; Buchwald, S. L. *Chem. Sci.* **2010**, *1*, 13–21.

(5) Fleckenstein, C. A.; Plenio, H. *Chem. Soc. Rev.* **2010**, *39*, 694–711.

(6) (a) Urgaonkar, S.; Nagarajan, M.; Verkade, J. G. *J. Org. Chem.* **2003**, *68*, 452–459. (b) Urgaonkar, S.; Verkade, J. G. *J. Org. Chem.* **2004**, *69*, 9135–9142. (c) Urgaonkar, S.; Xu, J.-H.; Verkade, J. G. *J. Org. Chem.* **2003**, *68*, 8416–8423.

(7) (a) Chartoire, A.; Frogneux, X.; Nolan, S. P. *Adv. Synth. Catal.* **2012**, *354*, 1897–1901. (b) Marion, N.; Nolan, S. P. *Acc. Chem. Res.* **2008**, *41*, 1440–1449. (c) Valente, C.; Çalimisis, S.; Hoi, K. H.; Mallik, D.; Sayah, M.; Organ, M. G. *Angew. Chem., Int. Ed.* **2012**, *51*, 3314–3332. (d) Zhu, L.; Ye, Y.-M.; Shao, L.-X. *Tetrahedron* **2012**, *68*, 2414–2420. (e) Fortman, G. C.; Nolan, S. P. *Chem. Soc. Rev.* **2011**, *40*, 5151–5169.

(8) Rodriguez, S.; Qu, B.; Haddad, N.; Reeves, D. C.; Tang, W.; Lee, H.; Krishnamurthy, D.; Senanayake, C. H. *Adv. Synth. Catal.* **2011**, *353*, 533–537.

(9) (a) Ogata, T.; Hartwig, J. F. *J. Am. Chem. Soc.* **2008**, *130*, 13848–13849. (b) Shen, Q.; Hartwig, J. F. *Org. Lett.* **2008**, *10*, 4109–4112. (c) Vo, G. D.; Hartwig, J. F. *J. Am. Chem. Soc.* **2009**, *131*, 11049–11061.

(10) Heravi, M. M.; Hashemi, M. *Tetrahedron* **2012**, *68*, 9145–9178.

(11) Suzuki, A. *J. Organomet. Chem.* **2002**, *653*, 83–90.

(12) (a) Du, Z.; Zhou, W.; Wang, F.; Wang, J.-X. *Tetrahedron* **2011**, *67*, 4914–4918. (b) Liu, C.; Ni, Q.; Hu, P.; Qiu, J. *Org. Biomol. Chem.* **2011**, *9*, 1054–1060. (c) Monguchi, Y.; Sakai, K.; Endo, K.; Fujita, Y.; Niimura, M.; Yoshimura, M.; Mizusaki, T.; Sawama, Y.; Sajiki, H. *ChemCatChem* **2012**, *4*, 546–558. (d) Qiu, J.; Wang, L.; Liu, M.; Shen, Q.; Tang, J. *Tetrahedron Lett.* **2011**, *52*, 6489–6491. (e) Silva, A. C.; Senra, J. D.; Aguiar, L. C. S.; Simas, A. B. C.; de Souza, A. L. F.; Malta, L. F. B.; Antunes, O. A. C. *Tetrahedron Lett.* **2010**, *51*, 3883–3885.

(13) (a) Martín, R.; Buchwald, S. L. *Acc. Chem. Res.* **2008**, *41*, 1461–1473. (b) Tang, W.; Capacci, A. G.; Wei, X.; Li, W.; White, A.; Patel, N. D.; Savoie, J.; Gao, J. J.; Rodriguez, S.; Qu, B.; Haddad, N.; Lu, B. Z.; Krishnamurthy, D.; Yee, N. K.; Senanayake, C. H. *Angew. Chem., Int. Ed.* **2010**, *49*, 5879–5883.

(14) Fu, G. C. *Acc. Chem. Res.* **2008**, *41*, 1555–1565.

(15) (a) Lundgren, R. J.; Stradiotto, M. *Chem.—Eur. J.* **2012**, *18*, 9758–9769. (b) Kozuch, S.; Shaik, S. *J. Mol. Catal. A—Chem.* **2010**, *324*, 120–126. (c) Diebolt, O.; Fortman, G. C.; Clavier, H.; Slawin, A. M. Z.; Escudero-Adán, E. C.; Benet-Buchholz, J.; Nolan, S. P. *Organometallics* **2011**, *30*, 1668–1676. (d) Jover, J.; Fey, N.; Harvey, J. N.; Lloyd-Jones, G. C.; Orpen, A. G.; Owen-Smith, G. J. J.; Murray, P.; Hose, D. R. J.; Osborne, R.; Purdie, M. *Organometallics* **2010**, *29*, 6245–6258. (e) Fey, N.; Orpen, A. G.; Harvey, J. N. *Coord. Chem. Rev.* **2009**, *253*, 704–722. (f) Schilz, M.; Plenio, H. *J. Org. Chem.* **2012**, *77*, 2798–2807.

(16) (a) Hill, L. L.; Moore, L. R.; Huang, R.; Craciun, R.; Vincent, A. J.; Dixon, D. A.; Chou, J.; Woltermann, C. J.; Shaughnessy, K. H. *J. Org. Chem.* **2006**, *71*, 5117–5125. (b) Hill, L. L.; Smith, J. M.; Brown, W. S.; Moore, L. R.; Guevara, P.; Pair, E. S.; Porter, J.; Chou, J.; Woltermann, C. J.; Craciun, R.; Dixon, D. A.; Shaughnessy, K. H. *Tetrahedron* **2008**, *64*, 6920–6934. (c) Hill, L. L.; Crowell, J. L.; Tutwiler, S. L.; Massie, N. L.; Hines, C. C.; Griffin, S. T.; Rogers, R. D.; Shaughnessy, K. H.; Grasa, G. A.; Johansson Seechurn, C. C. C.; Li, H.; Colacot, T. J.; Chou, J.; Woltermann, C. J. *J. Org. Chem.* **2010**, *75*, 6477–6488.

- (17) Tolman, C. A. *Chem. Rev.* **1977**, *77*, 313–348.
- (18) (a) DeVasher, R. B.; Spruell, J. M.; Dixon, D. A.; Broker, G. A.; Griffin, S. T.; Rogers, R. D.; Shaughnessy, K. H. *Organometallics* **2005**, *24*, 962–971. (b) an der Heiden, M.; Plenio, H. *Chem. Commun.* **2007**, 972–974. (c) an der Heiden, M. R.; Plenio, H.; Immel, S.; Burello, E.; Rothenberg, G.; Hoeflsoot, H. C. J. *Chem.—Eur. J.* **2008**, *14*, 2857–2866.
- (19) Ehrentraut, A.; Zapf, A.; Beller, M. *J. Mol. Cat. A: Chem.* **2002**, *182–183*, 515–523.
- (20) (a) Chartoire, A.; Frogneux, X.; Boreux, A.; Slawin, A. M. Z.; Nolan, S. P. *Organometallics* **2012**, *31*, 6947–6951. (b) Meiries, S.; Chartoire, A.; Slawin, A. M. Z.; Nolan, S. P. *Organometallics* **2012**, *31*, 3402–3409. (c) Organ, M. G.; Abdel-Hadi, M.; Avola, S.; Dubovyk, I.; Hadei, N.; Kantchev, E. A. B.; O'Brien, C. J.; Sayah, M.; Valente, C. *Chem.—Eur. J.* **2008**, *14*, 2443–2452. (d) Tu, T.; Fang, W.; Jiang, J. *Chem. Commun.* **2011**, *47*, 12358–12360.
- (21) Lee, D.-H.; Taher, A.; Hossain, S.; Jin, M.-J. *Org. Lett.* **2011**, *13*, 5540–5543.
- (22) Reddy, C. V.; Kingston, J. V.; Verkade, J. G. J. *Org. Chem.* **2008**, *73*, 3047–3062.
- (23) Wolfe, J. P.; Tomori, H.; Sadighi, J. P.; Yin, J.; Buchwald, S. L. J. *Org. Chem.* **2000**, *65*, 1158–1174.
- (24) Chartoire, A.; Lesieur, M.; Slawin, A. M. Z.; Nolan, S. P.; Cazin, C. S. J. *Organometallics* **2011**, *30*, 4432–4436.
- (25) Moore, L. R.; Western, E. C.; Craciun, R.; Spruell, J. M.; Dixon, D. A.; O'Halloran, K. P.; Shaughnessy, K. H. *Organometallics* **2008**, *27*, 576–593.
- (26) (a) Cauquis, G. *Compt. Rend.* **1958**, *247*, 1208–1211. (b) Cauquis, G. *Ann. Chim.* **1961**, *6*, 1161–1220. (c) Rigaudy, J.; Cauquis, G. *Compt. Rend.* **1956**, *242*, 2964–2967.
- (27) Littke, A. F.; Dai, C.; Fu, G. C. J. *Am. Chem. Soc.* **2000**, *122*, 4020–4028.
- (28) (a) Galardon, E.; Ramdeehul, S.; Brown, J. M.; Cowley, A.; Hii, K. K.; Jutand, A. *Angew. Chem., Int. Ed.* **2002**, *41*, 1760–1763. (b) Barrios-Landeros, F.; Carrow, B. P.; Hartwig, J. F. *J. Am. Chem. Soc.* **2009**, *131*, 8141–8154. (c) Barrios-Landeros, F.; Hartwig, J. F. *J. Am. Chem. Soc.* **2005**, *127*, 6944–6945.
- (29) Stambuli, J. P.; Incarvito, C. D.; Bühl, M.; Hartwig, J. F. *J. Am. Chem. Soc.* **2004**, *126*, 1184–1194.
- (30) (a) Sergeev, A. G.; Zapf, A.; Spannenberg, A.; Beller, M. *Organometallics* **2008**, *27*, 297–300. (b) Paul, F.; Patt, J.; Hartwig, J. F. *Organometallics* **1995**, *14*, 3030–3039.
- (31) Mitchell, E. A.; Jessop, P. G.; Baird, M. C. *Organometallics* **2009**, *28*, 6732–6738.
- (32) Yoshida, T.; Otsuka, S. *Inorg. Synth* **1990**, *28*, 113–119.
- (33) Tanaka, M. *Acta Crystallogr., Sect. C: Cryst. Struct. Commun.* **1992**, *C48*, 739–40.
- (34) Roy, A. H.; Hartwig, J. F. *J. Am. Chem. Soc.* **2003**, *125*, 13944–13945.
- (35) Chaudhari, K. R.; Wadawale, A. P.; Jain, V. K. *J. Organomet. Chem.* **2012**, *698*, 15–21.
- (36) Hooper, M. W.; Utsunomiya, M.; Hartwig, J. F. *J. Org. Chem.* **2003**, *68*, 2861–2873.
- (37) Barrios-Landeros, F.; Carrow, B. P.; Hartwig, J. F. *J. Am. Chem. Soc.* **2008**, *130*, 5842–5843.
- (38) (a) Christmann, U.; Pantazis, D. A.; Benet-Buchholz, J.; McGrady, J. E.; Maseras, F.; Vilar, R. *Organometallics* **2006**, *25*, 5990–5995. (b) Stambuli, J. P.; Kuwano, R.; Hartwig, J. F. *Angew. Chem., Int. Ed.* **2002**, *41*, 4746–4748. (c) Vilar, R.; Mingos, D. M. P.; Cardin, C. J. *J. Chem. Soc., Dalton Trans.* **1996**, 4313–4314.
- (39) Marion, N.; Ecarnot, E. C.; Navarro, O.; Amoroso, D.; Bell, A.; Nolan, S. P. *J. Org. Chem.* **2006**, *71*, 3816–3821.
- (40) Ishihara, K.; Nakagawa, S.; Sakakura, A. *J. Am. Chem. Soc.* **2005**, *127*, 4168–4169.
- (41) Gao, C.-Y.; Yang, L.-M. *J. Org. Chem.* **2008**, *73*, 1624–1627.
- (42) Tamano, M.; Nagai, Y.; Koketsu, J. *Nippon Kagaku Kaishi* **1987**, 684–7.
- (43) Wen, J.; Zhang, J.; Chen, S.-Y.; Li, J.; Yu, X.-Q. *Angew. Chem., Int. Ed.* **2008**, *47*, 8897–8900.
- (44) Lee, H. W.; Lam, F. L.; So, C. M.; Lau, C. P.; Chan, A. S. C.; Kwong, F. Y. *Angew. Chem., Int. Ed.* **2009**, *48*, 7436–7439.
- (45) Han, C.; Buchwald, S. L. *J. Am. Chem. Soc.* **2009**, *131*, 7532–7533.
- (46) Wolf, C.; Xu, H. *J. Am. Chem. Soc.* **2008**, *73*, 162–167.
- (47) Lombardo, M.; Chiarucci, M.; Trombini, C. *Green Chem.* **2009**, *11*, 574–579.
- (48) Stevens, P. D.; Fan, J.; Gardimalla, H. M. R.; Yen, M.; Gao, Y. *Org. Lett.* **2005**, *7*, 2085–2088.
- (49) APEX 2 AXScale and SAINT, version 2010, Bruker AXS, Inc., Madison, WI, 2010.
- (50) Sheldrick, G. M. *SHELXTL, Structure Determination Software Suite*, v.6.10, Bruker AXS, Madison, WI, 2001.